because of its potential for pharmaceutical vectors [9]. CPP-fused proteins are rapidly internalized by lipid raft-dependent macropinocytosis [11]. After internalization via the macropinocytotic pathway, the proteins are carried to macropinosomes, where most of them are then degraded [11]. Recent studies have shown that the ability to cross lipid bilayers and gain access to the cell interior of CPPs, especially poly-ariginine, is enhanced in the presence of the hydrophobic counteranion 4-(1-pyrenyl)-butyric acid (pyrenebutyrate, PB) [12,13]. The negatively charged counteranions and high hydrophobicity of PB can exert a great influence on the translocation behavior of arginine peptides in artificial membranes [12,13]. These features of the combination of poly-arginine and pyrenebutyrate are thought to be useful for the transdermal delivery of hydrophilic chemicals.

Hydroquinone (HQ) is a tyrosinase inhibitor and a hydrophilic antimelanogenesis compound used as an active ingredient in cosmetics and pharmaceuticals [14–16]. In the present study, we investigated whether protein transduction using poly-arginine in combination with PB was capable of delivering functional hydrophilic molecules and proteins into skin.

2. Materials and methods

2.1. Cell culture

Mouse B16 melanoma cells (B16-4A5) were provided by the European Collection of Cell Culture (ECACC). Cells were cultured in Dulbecco's modified Eagle's medium (D-MEM, Life Technologies, Grand Island, NY) with 10% fetal calf serum (Life Technologies), 100 U/ml penicillin, 100 U/ml streptomycin and 0.2% L-glutamine (Life Technologies). Cultures were maintained at 37 °C in 95% air and 5% CO_2 in a humidified incubator.

2.2. Peptide and HQ-11 synthesis

2.2.1. Cys(Npys)-Arg-Arg-Arg-Arg-Arg-Arg-Arg-Arg-Arg-Arg-Arg-NH_2

Peptide derivatives were assembled using an Applied Biosystems model 433 peptide synthesizer with Rink Amide MBHA Resin (0.34 mmol/g, 0.25 mmol) as the starting solid support. The protected peptide resin was treated with a deprotecting reagent [TFA-TIS-H_2O (95/2.5/2.5/, v/v)] at room temperature for 2 h. The crude S-Npys derivatives were isolated and purified by RP-HPLC. The purified Npys was used for the final disulfide formation procedure.

2.2.2. Cys[$(OH)_2C_6H_4S$-]-Arg-Arg-Arg-Arg-Arg-Arg-Arg-Arg-Arg-Arg-Arg-NH_2·11TFA

HQ was conjugated with poly-arginine peptides as shown in Fig. 1. To an aqueous solution (1.2 ml) of Cys(Npys)-11Arg-NH_2 (60 mg) was added $(OH)_2C_6H_4SH$(2-mercaptohydroquinone, 3.6 mg, 0.8 eq) with stirring at room temperature overnight under an Argon gas atmosphere. After the reaction was over, the reaction mixture was directly subjected RP-HPLC [YMC ODS column (30 × 250 mm, 0.1%TFA/H_2O)]. The desired peptide was obtained as a TFA salt (25 mg), as confirmed by RP-HPLC and Mass spectral analysis. Cys[$(OH)_2C_6H_4S$-]-Arg-Arg-Arg-Arg-Arg-Arg-Arg-Arg-Arg-Arg-Arg-NH_2·11TFA; Mol wt: 3232.6 as TFA salt, C75H144N46O14S2 MW: 1978.4, MS analysis : m/z 660.4(M 3H)3, m/z 495.6([M 4H]4), Purity: 94.5%.

2.3. Protein/peptide transduction into cells

The transduction of protein and peptide into cells was carried out as described previously [12]. Briefly, cells were plated onto dishes (diameter 3 cm) and incubated in D-MEM containing 10% FBS (Life Technologies), 1% penicillin and streptomycin for 48 h in a humidified atmosphere containing 5% CO_2. After removal of the medium, the cells were washed twice with PBS and incubated with 50 μM 4-(1-pyrenyl)-

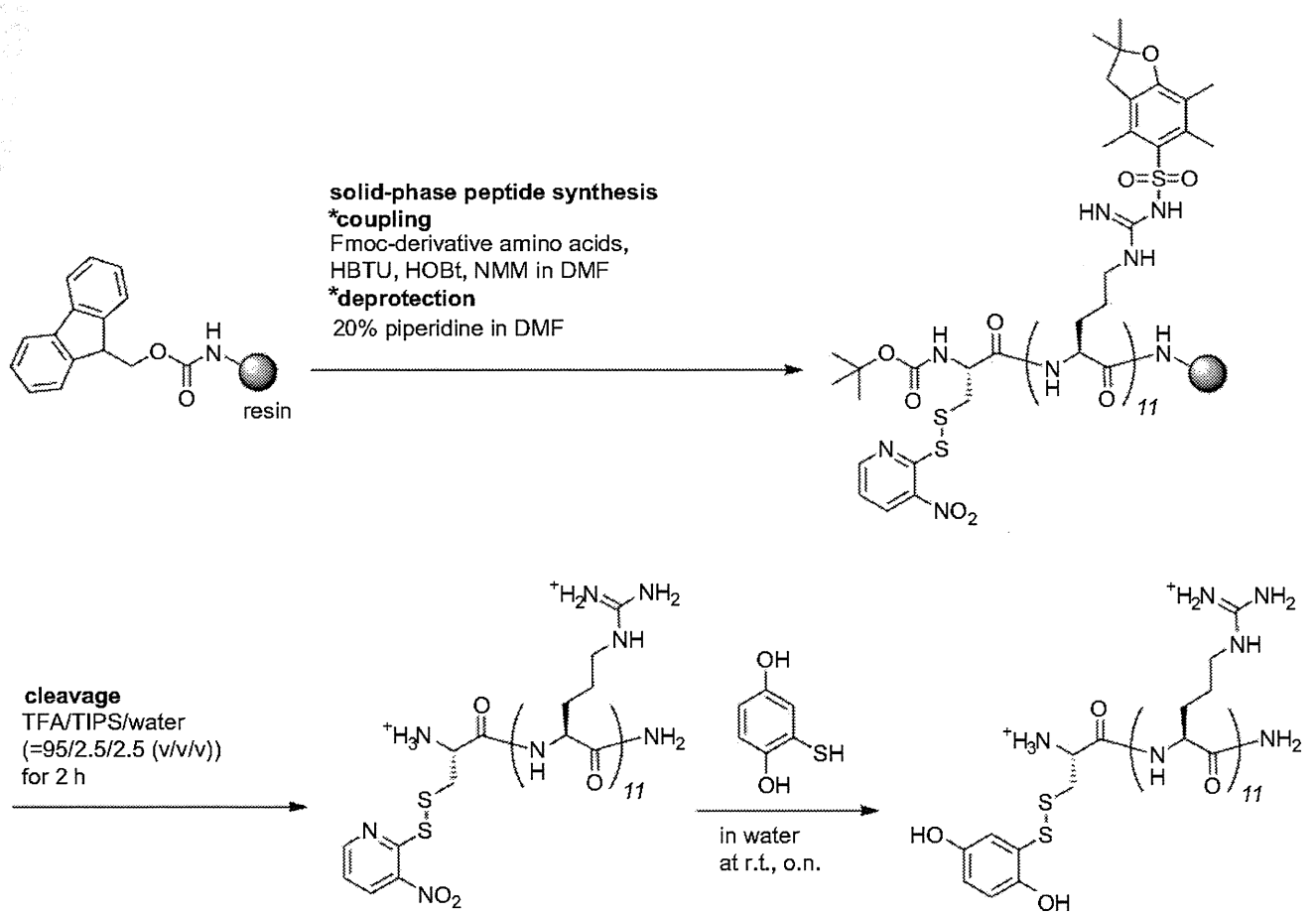

Fig. 1. The schema of HQ-11R synthesis.

butyric acid (PB, Sigma–Aldrich, St. Louis, MO) in PBS for 2 min at 37 °C. Cells were then replaced with new PBS and protein or peptide dissolved in PBS was added. After 20 min, the cells were washed twice with PBS and incubated further in new medium for the period indicated.

2.4. Cell viability assay

Cell viability was determined using a CellTiter-Glo® Luminescent Cell Viability Assay kit (Promega, Madison, WI) following the manufacturer's instructions. After the application of HQ and HQ-11R, B16 cells (1×10^3 per well) seeded onto 96-well plates were cultured in D-MEM containing 10% fetal bovine serum, and 1% penicillin and streptomycin for 24 h. After being washed with PBS, the cells were placed in fresh D-MEM and incubated further for 24, 48 and 72 h. Cell viability was measured using a CellTiter-Glo® Luminescent Cell Viability Assay kit with microplate luminometer device [MicroLumat Plus LB 96V, Berthold technologies, (Bad Wildbad, Germany)].

2.5. Expression and purification of recombinant forms of EGFP and EGFP-11R

The recombinant forms of enhanced green fluorescent protein (EGFP) and eleven poly-arginine-fused EGFP (EGFP-11R) were produced as described previously [17].

2.6. Confocal laser microscopic analysis

Cells (2×10^5) were plated onto 35-mm-diameter glass-bottomed dishes (Iwaki, Tokyo, Japan) coated with laminin and cultured for 48 h. Cells were preincubated with 50 μm PB or PBS for 2 min at 37 °C. 20 min after the transduction of 5 μM EGFP and EGFP-11R, the cells were washed twice with PBS and the medium was replaced with D-MEM containing 10% (v/v) calf serum, 1% penicillin and streptomycin. The EGFP signals in living cells were observed using a confocal laser microscope (FV300, Olympus, Tokyo, Japan) equipped with a 60× objective lens at 0.5, 2, 4 and 8 h after protein transduction.

2.7. Western blotting analysis

Western blotting was carried out at high stringency, essentially as described previously [18]. The harvested cells were lysed by a sonicator in a boiled buffer containing 1% SDS. The cell lysate (50 μg) was subjected to SDS-PAGE and transferred to nitrocellulose membranes (Hybond ECL, Amersham Biosciences). The blots were probed with primary antibodies against tyrosinase (1:100) (Abcam, Tokyo, Japan). Immunoreactive bands were visualized by enhanced chemiluminescence using ECL plus (GE Healthcare UK Ltd, Buckinghamshire, England) and Bio-Rad Versadoc (Model 5000, Bio-Rad Laboratories, Inc., Hercules, CA).

2.8. Measurement of melanin contents

Melanin content was measured described previously [19]. Briefly, B16-4A5 cells dissolved in 1 ml of 5% trichloroacetic acid (TCA) were incubated on ice for 10 min. After centrifugation, the precipitate was dissolved in 2 ml of EtOH-ether (3:1) and centrifuged. The precipitate was resuspended in 2 ml of ether, and centrifuged for 10 min. Finally, the precipitate was air-dried, and resuspended in 0.5 ml of 2 N NaOH at 80 °C for 1 h. The absorbance at 415 nm was measured.

2.9. Topical application of EGFP-11R and EGFP

The hair from the back of adult guinea pigs (Female Weiser-Maples, SHIMIZU Laboratory Supplies, Kyoto, Japan) weighing 450–500 g was removed carefully using depilatory cream 24 h before the study. All procedures of animal experiments were approved by the Animal Ethics Committee of Okayama University (OKU-2008019). Areas of 4.0 cm^2 were marked on the dorsal trunk of the animals using a template. For topical treatment of EGFP-11R, PB in propylene glycol [a mixture of 1 μl of PB (50 mM) and 99 μl of propylene glycol] was pre-applied on the skin. After 5 min, 11R-EGFP [a mixture of 25 μl of 11R-EGFP (50 μM) and 25 μl of propylene glycol] was applied to the same region. As a control, EGFP or EGFP-11R [a mixture of 25 μl of 11R-EGFP or EGFP (50 μM each) and 25 μl of propylene glycol] was applied on the skin of same guinea pigs. Skin sections were obtained at 0.5, 2, 4, and 8 h after the topical applications with a 3-mm dermapunch (Maruho, Osaka, Japan). Excised skin samples were immediately frozen in Optimal Cutting Temperature compound (Sakura Finetek, Japan) and sequentially sectioned at a thickness of 10 μm. The sections were fixed with 4% PFA in 0.1 M phosphate buffer (pH 7.4) for 15 min. After being washed with PBS, the sections were incubated with Hoechst 33258 (1 μg/ml) for 5 min, and viewed using a confocal microscope (FluoView™ FV300, Olympus, Tokyo, Japan).

2.10. UV-induced pigmentation and topical treatment in vivo

Hyperpigmentation was induced on the backs of brown guinea pigs by the modification of a method as described previously [20]. Four separate areas (2 cm × 3 cm square) on the back were shaved and exposed to UV from Model UVM-57 lamps (Funakoshi, Tokyo, Japan), The total dose of UV was 15 mJ/cm^2 per day. Animals were exposed five days a week for two consecutive weeks (Fig. 2). Two days after the last UV irradiation, HQ (a mixture of 50 μl of 1 mM HQ and 50 μl of propylene glycol) was applied to the tanning lesion. HQ-11R and HQ-GLHFPHIYVRD (a mixture of 50 μl of 1 mM HQ or HQ-peptide and 50 μL of propylene glycol) were applied to the tanning lesion 5 min after pre-treatment with PB (a mixture of 1 μl of 50 mM PB and 99 μl of propylene glycol). Guinea pigs were treated with HQ and HQ-peptides once a day, 5 days a week, for a total of 10 days (Fig. 2). Three days after the last treatment, the animals were sacrificed and skin samples were taken with a 3-mm dermapunch (Maruho, Japan). As a control, the guinea pigs were received 100 μl of propylene glycol.

2.11. Histology study

Under general euthanasia, skin was removed and fixed in 4% paraformaldehyde in PBS. After paraffin processing, paraffin, embedded tissue sections 4.5 μm thick were processed for light microscopic examination. A hematoxylin and eosin (H&E) stain was used for studying the general histopathological changes in the skin. Melanin pigments were visualized with Fontana-Masson silver staining followed by eosin background staining as described previously [21]. Melanin-positive cells were counted in a 500 × 400 μm area in 20 different fields.

2.12. Statistical analysis

Data are shown as the mean ± S.D. Data were analyzed using either Student's *t*-test to compare two conditions or ANOVA followed by planned comparisons of multiple conditions, and $P < 0.05$ was considered to be significant.

3. Results

3.1. Effect of poly-arginine-fused HQ (HQ-11R) with 1-pyrenebutyric acid (PB) on the viability of B16-4A5 melanoma cells

To investigate the cell toxicity of HQ-11R with PB in B16-4A5, a cell line of mouse melanoma, the cells were incubated with each concentration of HQ and HQ-11R. When the cells were incubated with 0.5 and 5.0 μM of HQ alone or of HQ-11R with 50 μM PB μM PB, viability was the same as that of the control after 24, 48 and 72 h (Fig. 3A), suggesting that neither HQ and nor HQ-11R with PB had cell toxicity when used at concentrations of 0.5 and 5 μM. Viability was significantly inhibited when the cells were treated with 50 μM of HQ-11R. However, 50 μM of HQ also inhibited cell viability the same as HQ-11R (Fig. 3A), suggesting the inhibitory effect to be due to HQ.

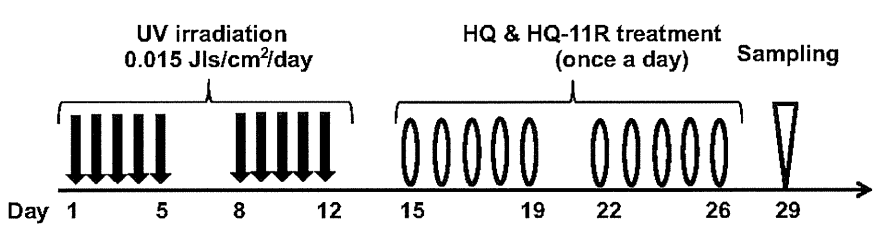

Fig. 2. Time schedule of UV irradiation and applications of HQ and HQ-11R.

3.2. Inhibitory effect of HQ-11R on melanin content

To investigate whether HQ-11R inhibited melanogenesis, B16-4A5 cells were incubated with 10, 20 and 30 μM of HQ and HQ-11R and melanin content was measured. Both HQ and HQ-11R dose-dependently inhibited melanin synthesis (Fig. 3B). The inhibitory effect of HQ-11R was the same as that of HQ (Fig. 3B). HQ fused with a control peptide (HQ-GLHFPHIVRD), which consisted of eleven amino acids and had no ability to penetrate cells, did not inhibit melanin synthesis when used at 10 and 20 μM (Fig. 3B). HQ-

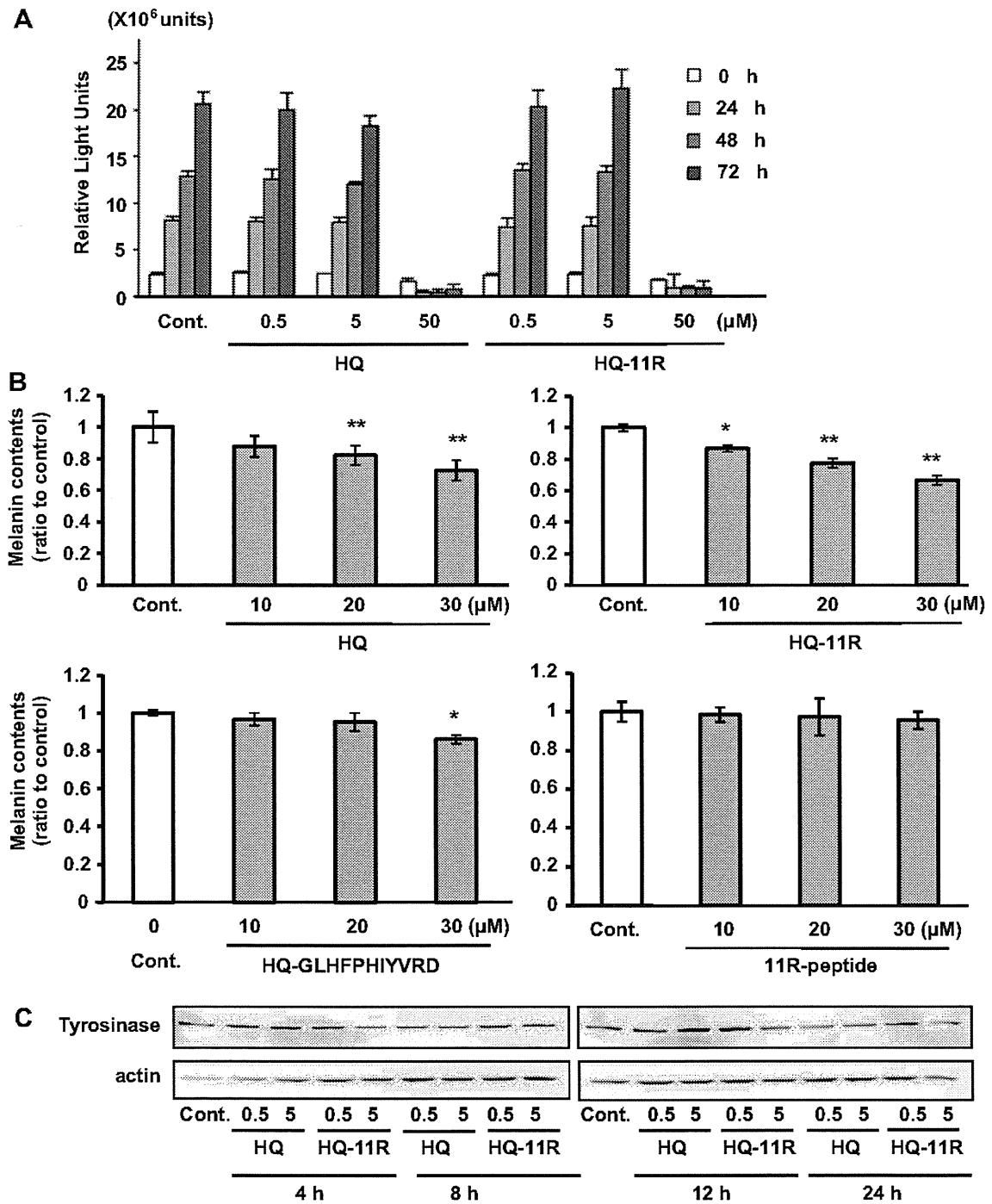

Fig. 3. Comparison of the inhibitory effect on melanin synthesis between hydroquinone (HQ) and eleven poly-arginine-fused HQ (HQ-11R) in B16-4A5 melanoma cells. (A) Cell viability was measured by the CellTiter-Glo Luminescent Cell Viability assay. B16-4A5 cells were treated with 10, 20 and 30 μM of HQ alone or HQ-11R in the presence of PB for the periods indicated. Control cells (Cont.) were intact cells. Data are represented as the mean ± SD. $n = 6$ each. (B) Measurement of melanin contents in the cells treated with 10, 20 and 30 μM of HQ, HQ-11R, HQ-GLHFPHIYBRD and 11R-peptide for 24 h. Data are represented as the mean ± SD. $n = 6$ each. $^{*}P < 0.05$, $^{**}P < 0.01$ (C) Effect of HQ and HQ-11R on tyrosinase levels in B16-4A5 cells. The cells were treated with HQ alone and HQ-11R with PB for the periods indicated. The cells were harvested at each time point and the lysates were used for Western blotting.

GLHFPHIVRD inhibited melanin synthesis at 30 μM but its effect was weaker than HQ-11R and HQ alone (Fig. 3B). The 11R-peptide without HQ had no effect on melanin synthesis (Fig. 3B). HQ is a potent inhibitor of tyrosinase, a key enzyme in melanin synthesis, but did not affect the expression or degradation of the enzyme [22,23]. Some tyrosinase inhibitors display a hypopigmenting effect through post-transcriptional control of the tyrosinase. Linoleic acid decreases the amount of tyrosinase through increased tyrosinase ubiquitination and degradation by the proteasome [23]. *N*-Acetyl-glucosamine reduced melanin synthesis through the inhibition of

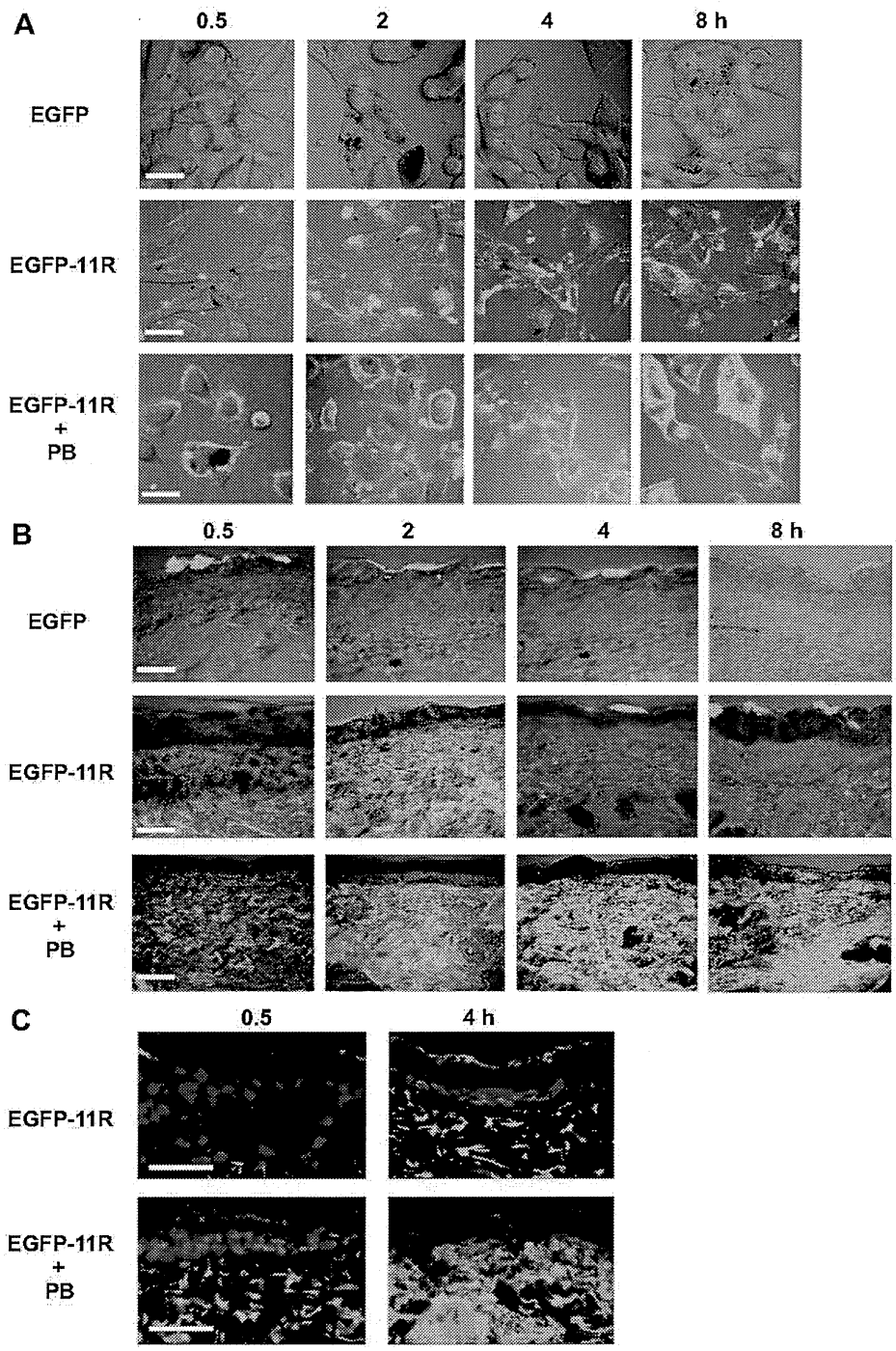

Fig. 4. Transdermal transduction of EGFR-11R with PB. (A) Time-dependent transduction of EGFR-11R with or without PB in B16-4A5 cells. The cells were treated with 1 μM EGFP-11R (EGFP-11R). After pre-treatment with PB for 5 min, 1 μM EGFP was added (EGFP-11R + PB). The signals were observed by confocal microscopy at each time point. Bars = 10 μm. (B) Time-dependent transdermal delivery of EGFP-11R. EGFP and EGFP-11R with/without PB were applied on the skin of guinea pigs. Skin sections were obtained at each time point and EGFP signals were observed with a confocal microscope. Bars = 200 μm. (C) The distribution of EGFP-11R in the epidermis and dermis of guinea pigs. EGFP-11R was applied with or without PB. The skin sections were counter-stained with Hoechst 33258 (blue). Bars = 50 μm. (For interpretation of the references to color in this figure legend, the reader is referred to the web version of this article.)

tyrosinase glycosylation [24]. To investigate the possibility that the inhibitory effect of HQ-11R on melanin synthesis was due to the post-transcriptional control of tyrosinase, tyrosinase levels were examined in B16-4A5 cells treated with HQ and HQ-11R. Neither HQ nor HQ-11R affected the protein level (Fig. 3C), suggesting that HQ-11R may inhibit melanin synthesis through the inhibition of tyrosinase activity.

3.3. Transdermal delivery of EGFP-11R with PB

Next, the efficiency of the delivery of EGFP fused with 11R (EGFP-11R) in B16-4A5 cells was examined. EGFP without 11R was not observed in the cells (Fig. 4A). The signals were observed in almost all of the cells 30 min after the addition of EGFP-11R regardless of PB (Fig. 4A). Strong signals were observed 2, 4 and

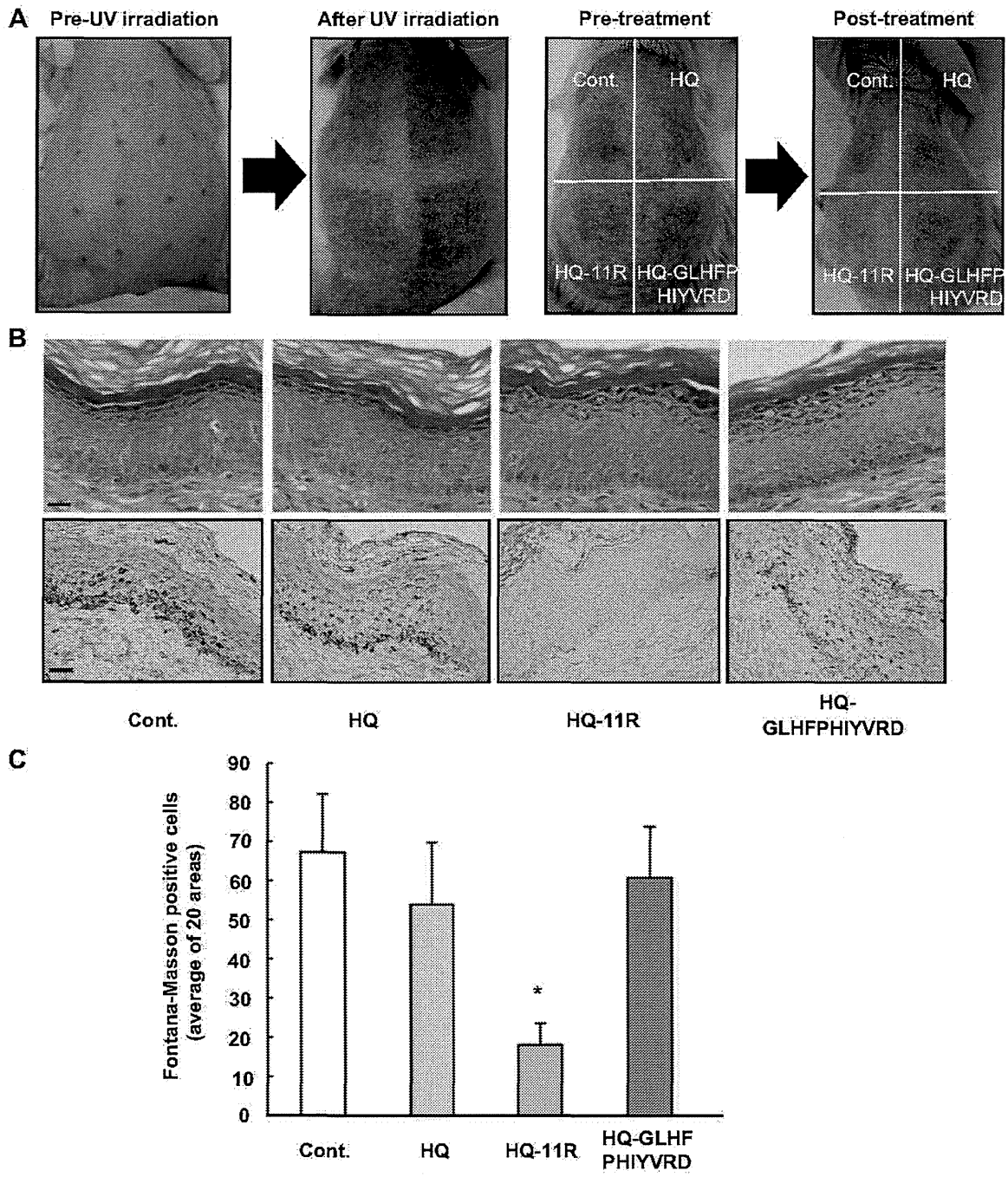

Fig. 5. Inhibitory effect of HQ-11R on UV-induced pigmentation in guinea pig skin. (A) A representative image of the back of the guinea pigs pre-radiation, post-radiation, and pre-treatment and post-treatment with HQ, HQ-non CPP peptide and HQ-11R. Each area is 2 cm × 2 cm square. (B) Biopsy specimens from HQ-, HQ-11R- or HQ-GLHFPHIYVRD-treated guinea pig skin after 10 days of topical application were examined by H.E. staining (upper panel) and Fontana-Masson silver staining (lower panel). Bars = 50 μm. (C) Number of cells positive for Fontana-Masson stain. The positive cells were counted in a 500 × 400 μm area in 20 different fields. *$P < 0.01$.

8 h after the transduction regardless of PB (Fig. 4A). Preincubation of PB did not affect the efficiency of EGFP-11R transduction in the cells (Fig. 4A).

We next examined the effectiveness of the topical application of EGFP-11R. When EGFP was topically applied, the signals were only observed on the surface of the skin (Fig. 4B). The topical application of EGFP-11R without PB delivered the protein into the dermis (Fig. 4B). However, signals were not observed in the epidermal layer (Fig. 4B). Strong signals in the epidermal layer were observed 0.5 and 2 h after the application but the signals were faint at 4 and 8 h. When EGFP-11R was applied with PB, strong signals were detected in both epidermis and dermis 0.5 and 2 h after the application (Fig. 4B). Moreover, the signals were spread out more and stronger in both layers after 4 and 8 h (Fig. 4B).

To investigate whether EGFP-11R was delivered in the cells of the epidermis and dermis, the skin sections were counter-stained with Hoechst (Fig. 4C). Most EGFP signals did not overlap with Hoechst staining when EGFP-11R was applied without PB, suggesting that 11R-EGFP was delivered in the space of the epidermal layer (Fig. 4C). In contrast, when EGFP-11R was applied with PB, the signals overlapped with Hoechst staining in the cells of both epidermis and dermis 4 h after the application (Fig. 4C).

3.4. Inhibitory effect of HQ-11R on UV-induced pigmentation in guinea pig skin

The whitening effect of HQ-11R was examined using UV-induced pigmentation of brown guinea pig skin. After UV irradiation for 10 days, guinea pigs were topically treated with HQ, and HQ-11R and HQ-GLHFPHIYVRD with PB for 10 days (Figs. 2 and 5A). The treatments did not induce abnormal morphological changes in the epidermis and dermis (Fig. 5B). The HQ application tended to decrease levels of melanin but not significant (Fig. 5B and C). HQ-11R significantly reduced melanin levels in the basal cell layer of the epidermis whereas HQ-GLHFPHIYVRD lacking the ability to penetrate cells had no effect on melanin levels in the epidermis (Fig. 5C).

4. Discussion

Protein transduction method using CPPs such as 11R is widely accepted as useful for the delivery of proteins, peptides and cell-impermeable molecules into cells [25]. Previous studies have showed the effective transdermal skin delivery of proteins and peptides employing CPPs including Tat (Trans-activating transcriptional activator), YARA, WLR, and 9R peptides [26–29]. In the present study, we also showed that protein transduction method using 11R was valuable for the transdermal delivery of EGFP and HQ. However, EGFP-11R without PB was not delivered into cells of the epidermis although signals were observed in the layer. These results suggest that protein transduction using CPPs is capable of increasing the penetration of skin by proteins but most proteins delivered topically do not enter or function in cells of the epidermis and dermis. In contrast, EGFP-11R was delivered to cells of the epidermis and dermis and HQ-11R reduced melanin levels in the basal cell layer of epidermis when applied in combination with 4-(1-pyrenyl)-butyric acid (PB), suggesting that PB enhances the intracellular delivery of proteins and hydrophilic molecules delivered transdermally. The molecular mechanism by which CPP-fused proteins cross the cell membrane is different with that without PB. CPP fusion proteins are internalized rapidly by lipid raft-dependent macropinocytosis [11]. In contrast, the negatively charged counteranions and high hydrophobicity of PB can exert a great influence on the translocation behavior of arginine peptides in artificial membranes [12,13]. Endogenous mechanism such as macropinocytosis and endocytosis are not necessary for the intracellular delivery of poly-arginine fusion proteins when applied with PB. The artificial membrane penetration may be convenient for the transdermal delivery of poly-arginine fusion proteins.

The backbone of PB is a pyrene, a polycyclic aromatic hydrocarbon consisting of four fused benzene rings and it contains a hydrophilic carboxylic acid. The structure is similar with benzopyrene, which consists of five benzene rings. Benzopyrene is found in coal tar and cigarette smoke, and shows an evidence of carcinogenicity in lung cells [30]. Therefore, PB is misunderstood to have toxicity. However, a previous study showed that PB had no significant cytotoxicity [12]. In the present study, moreover, PB did not affect the growth of B16-4A5 nor cause dermatitis in guinea pigs. These results suggest protein transduction using 11R and PB to be safe as a transdermal delivery method. However, further study is needed.

A previous study showed that bioactive proteins were transdermally delivered by non-covalently associated poly-arginine peptides [27]. We also examined whether HQ non-covalently associated with 11R was delivered in the dermis and epidermis of guinea pigs when applied with 11R. However, HQ was not delivered in the skin (data not shown). These results suggest that transdermal delivery by non-covalently associated poly-arginine peptides may be suitable for proteins and peptides but not low molecules.

In conclusion, a topical approach using poly-arginine in combination with PB was proven to be beneficial for the delivery of proteins and hydrophilic drugs. HQ-11R is a candidate for a skin-whitening agent with the advantages of strong tyrosinase inhibition, effective penetration of the skin, and relatively little cytotoxicity.

5. Conclusion

The present results showed that a poly-arginine (11R) with pretreatment of PB was effective at topical delivering system to enter or function in cells of the epidermis and dermis. It appears that our system can be used to deliver many kinds of proteins and whitening-agents into g transcription factors into various cells. *In vivo* topical protein transduction method with pyrenbutyrate may overcome the disadvantages of previous methods and become a promising modality in dermatological field and cosmetics industry.

Acknowledgments

We thank A. Ueda for technical assistance. This work was supported by a Grant-in-aid for Scientific Research from the Ministry of Education, Science, Sports and Culture of Japan and by a Grant-in-aid for Scientific Research from the Ministry of Health, Labor and Welfare of Japan.

References

[1] Liu CH, Chang FY. Development and characterization of eucalyptol microemulsions for topic delivery of curcumin. Chem Pharm Bull 2011;59:172–8.
[2] Kogan A, Garti N. Microemulsions as transdermal drug delivery vehicles. Adv Colloid Interface Sci 2006;123–126:369–85.
[3] Matsui H, Tomizawa K, Lu YF, Matsushita M. Protein therapy: in vivo protein transduction by polyarginine (11R) PTD and subcellular targeting delivery. Curr Protein Pept Sci 2003;4:151–7.
[4] Tomoda K, Terashima H, Suzuki K, Inagi T, Terada H, Makino K. Enhanced transdermal delivery of indomethacin-loaded PLGA nanoparticles by iontophoresis. Colloids Surf B Biointerfaces 2011;88:706–10.
[5] Shah VP, Behl CR, Flynn GL, Higuchi WI, Schaefer H. Principles and criteria in the development and optimization of topical therapeutic products. J Pharm Sci 1992;81:1051–4.
[6] Nino M, Calabrò G, Santoianni P. Topical delivery of active principles: the field of dermatological research. Dermatol Online J 2010;16:4.

[7] Korting HC, Stolz W, Schmid MH, Maierhofer G. Interaction of liposomes with human epidermis reconstructed in vitro. Br J Dermatol 1995;132:571–9.
[8] Schwarze SR, Hrusk KA, Dowdy SF. Protein transduction: unrestricted delivery into all cells? Trends Cell Biol 2000;10:290–5.
[9] Futaki S, editor. Special theme issue on membrane permeable peptide vectors: chemistry and functional design for the therapeutic application, vol. 60; 2008. p. 447–614. Adv drug delivery Rev.
[10] Joliot A, Prochiantz A. Transduction peptides: from technology to physiology. Nat Cell Biol 2004;6:189–96.
[11] Wadia JS, Stan RV, Dowdy SF. Transducible TAT-HA fusogenic peptide enhances escape of TAT-fusion proteins after lipid raft macropinocytosis. Nat Med 2004;10:310–5.
[12] Takeuchi T, Kosuge M, Tadokoro A, Sugiura Y, Nishi M, Kawata M. Direct and rapid cytosolic delivery using cell-penetrating peptides mediated by pyrenebutyrate. ACS Chem Biol 2006;1:299–303.
[13] Guterstam P, Madani F, Hirose H, Takeuchi T, Futaki S, El Andaloussi S. Elucidating cell-penetrating peptide mechanisms of action for membrane interaction, cellular uptake, and translocation utilizing the hydrophobic counter-anion pyrenebutyrate. Biochim Biophys Acta 2009;1788:2509–17.
[14] Westerhof W, Kooyers TJ. Hydroquinone and its analogues in dermatology–a potential health risk. J Cos Dermatol 2005;4:55–9.
[15] Nordlund JJ, Grimes PE, Ortonnes JP. The safety of hydroquinone. J Eur Acad Dermatol Venereol 2006;20:781–7.
[16] Chen YR, Y-Y R, Lin TY, Huang CP, Tang WC, Chen ST. Identification of an alkylhydroquinone from Rhus succedanea as an inhibitor of tyrosinase and melanogenesis. J Agric Food Chem 2009;57:2200–5.
[17] Matsushita M, Tomizawa K, Moriwaki A, Li ST, Terada H, Matsui H. A high-efficiency protein transduction system demonstrating the role of PKA in long-lasting long-term potentiation. J Neurosci 2001;21:6000–7.
[18] Takenobu T, Tomizawa K, Matsushita M, Li ST, Moriwaki A, Lu YF. Development of p53 protein transduction therapy using membrane-permeable peptides and the application to oral cancer cells. Mol Cancer Ther 2002;1:1043–9.
[19] Fujita H, Motokawa T, Katagiri T, Yokota S, Yamamoto A, Himeno M. Inulavosin, a melanogenesis inhibitor, leads to mistargeting of tyrosinase to lysosomes and accelerates its degradation. J Invest Dermatol 2009;129:1489–99.
[20] Kim JH, Baek SH, Kim DH, Choi TY, Yoon TJ, Hwang JS. Downregulation of melanin synthesis by haginin A and its application to in vivo lightening model. J Invest Dermatol 2008;128:1227–35.
[21] Park KT, Ki JK, Hwang D, Yoo Y, Lim YH. Inhibitory effect of mulberroside A and its derivatives on melanogenesis induced by ultraviolet B irradiation. Food Chem Toxicol 2011;49:3038–45.
[22] Maeda K, Fukuda M. Arbutin: mechanism of its depigmenting action in human melanocyte culture. J Pharmacol Exp Ther 1996;276:765–9.
[23] Kim H, Choi HR, Kim DS, Park KC. Topical hypopigmenting agents for pigmentary disorders and their mechanisms of action. Ann Dermatol 2012;24:1–6.
[24] Hwang JS, Lee HY, Lim TY, Kim MY, Yoon TJ. Disruption of tyrosinase glycosylation by N-acetylglucosamine and its depigmenting effects in guinea pig skin and in human skin. J Dermatol Sci 2011;63:199–201.
[25] van den Berg A, Dowdy SF. Protein transduction domain delivery of therapeutic macromolecules. Curr Opin Biotechnol 2011;22:888–93.
[26] Rothbard JB, Garlington S, Lin Q, Kirschberg T, Kreider E, Mcgrane PL. Conjugation of arginine oligomers to cyclosporin A facilitates topical delivery and inhibition of inflammation. Nat Med 2000;6:1253–7.
[27] Hou YW, Chan MH, Hsu HR, Liu BR, Chen CP, Chen HH. Transdermal delivery of proteins mediated by non-covalently associated arginine-rich intracellular delivery peptides. Exp Dermatol 2007;16:999–1006.
[28] Lopes LB, Furnish E, Komalavilas P, Seal BL, Panitch A, Bentley MV. Enhanced skin penetration of P20 phosphopeptide using protein transduction domains. Eur J Pharm Biopharm 2008;68:441–5.
[29] Kang MJ, Eum JY, Park SH, Kang MH, Park KH, Choi SE. Pep-1 peptide-conjugated elastic liposomal formulation of taxifolin glycoside for the treatment of atopic dermatitis in NC/Nga mice. Int J Pharm 2010;402:198–204.
[30] Denissenko MF, Pao A, Tang M, Pfeifer GP. Preferential formation of benzo[a]pyrene adducts at lung cancer mutational hotspots in P53. Science 1996;274:430–2.

Biomaterials 33 (2012) 4665–4672

Contents lists available at SciVerse ScienceDirect

Biomaterials

journal homepage: www.elsevier.com/locate/biomaterials

A protein transduction method using oligo-arginine (3R) for the delivery of transcription factors into cell nuclei

Takashi Hitsuda [a,1], Hiroyuki Michiue [a,*,1], Mizuki Kitamatsu [c], Atsushi Fujimura [a], Feifei Wang [a], Takahiro Yamamoto [c], Xiao-Jian Han [a], Hiroshi Tazawa [b,d], Atsuhito Uneda [a], Iori Ohmori [a], Tei-ichi Nishiki [a], Kazuhito Tomizawa [e], Hideki Matsui [a]

[a] Department of Physiology, Okayama University Graduate School of Medicine, Dentistry and Pharmaceutical Sciences, 2-5-1 Shikata-cho, Okayama 700-8558, Japan
[b] Department of Gastroenterological Surgery, Okayama University Graduate School of Medicine, Dentistry and Pharmaceutical Sciences, 2-5-1 Shikata-cho, Okayama 700-8558, Japan
[c] Department of Bioscience and Biotechnology, Okayama University Graduate School of Natural Science and Technology, 3-1-1 Tsushimanaka, Kita-Ku, Okayama 700-0082, Japan
[d] Center for Gene and Cell Therapy, Okayama University Hospital, 2-5-1 Shikata-cho, Okayama 700-8558, Japan
[e] Department of Molecular Physiology, Faculty of Life Sciences, Kumamoto University, Kumamoto 860-8558, Japan

ARTICLE INFO

Article history:
Received 29 November 2011
Accepted 27 February 2012
Available online 30 March 2012

Keywords:
Protein transduction
eGFP
p53
Arginine
Drug delivery
TAT

ABSTRACT

Protein transduction with cell-penetrating peptides such as poly-arginine and HIV TAT peptides is widely used to deliver proteins, peptides, siRNA and biologically active compounds. It has been thought that poly-arginine peptides transduce proteins in a manner dependent on the number of arginine residues and oligo-peptides such as three arginines (3R) are ineffective. Here we showed that 3R-fused proteins were effectively delivered and functioned in cells co-treated with pyrenebutyrate, a counteranion bearing an aromatic hydrophobic moiety. Little 3R was transduced in glioma cells without pyrenebutyrate whereas the oligo-arginine was effectively delivered with pyrenebutyrate. Enhanced green fluorescence protein (eGFP) fused with 3R was effectively delivered into various kinds of cells including primary cultured cells and suspended cells in the presence of pyrenebutyrate. p53 fused with 3R (3R-p53) was delivered into glioma cells without pyrenebutyrate but could not be translocated into the nucleus. In contrast, 3R-p53 was observed in nuclei of glioma cells when co-applied with pyrenebutyrate. Although 3R-p53 was delivered less effectively than 11R-p53 with pyrenebutyrate, its transcriptional activity was higher than that of 11R-p53. Moreover, a single administration of 3R-p53 with pyrenebutyrate significantly inhibited the growth of cancer cells. These results suggest protein transduction using an oligo-arginine (3R) with pyrenebutyrate to be a good tool for the delivery of functional transcription factors and a promising method of treating cancer.

1. Introduction

Protein transduction using short peptides such as protein transduction domains (PTDs) or cell-penetrating peptides (CPPs) is a good tool for delivering exogenous peptides, proteins, siRNAs, PNA, magnetic beads, small molecules and many biological compounds *in vitro* and *in vivo* [1–6]. The PTD of the Tat protein, which contains a high proportion of arginine and lysine residues, was identified as responsible for the ability to penetrate the plasma membrane [7–9]. Moreover, poly-arginine peptides, 6–12 residues long, have the same transduction activity as PTDs [10–12]. Eight (8R) and eleven (11R) arginine-long peptides carry biological compounds more effectively than other CPPs and PTDs [10–12]. However, poly-arginine peptides consist of basic amino acids and are positively charged [9]. This may cause the functional loss of transcription factors and proteins in which acidic amino acids are abundant because of interaction with DNA and the acidic amino acids. In fact, some transcription factors fused with poly-arginine peptides do no function even when delivered into cells [13,14].

p53 is a transcription factor and tumor suppressor [15]. We previously showed that 9R- and 11R-fused p53 proteins (p53-9R and p53-11R) effectively penetrated the plasma membrane of cancer cells [13,14]. Both proteins induce the activity of the p21/WAF1 promoter and inhibit the proliferation of cancer cells [16]. However, a high concentration (>10 μM) and repeated

* Corresponding author. Tel.: +81 86 235 7105; fax: +81 96 373 5052.
E-mail address: hmichiue@md.okayama-u.ac.jp (H. Michiue).
[1] These authors equally contributed.

0142-9612/$ – see front matter © 2012 Elsevier Ltd. All rights reserved.
doi:10.1016/j.biomaterials.2012.02.049

administration of p53-11R are needed for transcriptional activation and inhibition of the growth of cancer cells [14]. One possibility is that long poly-arginine peptides affect the transcriptional activity. Fusion of an oligo-arginine domain such as 3R may overcome this problem if the domain is capable of protein transduction. In the present study, we developed a protein transduction method using 3R-fused p53 in combination with pyrenebutyrate, a counteranion bearing an aromatic hydrophobic moiety and a mediator of direct and rapid cytosolic delivery of oligo-arginine-fused proteins.

2. Materials and methods

2.1. Peptide synthesis

Fluorescent TMR-conjugated poly-arginine peptides (3R, 5R, 7R, 9R, and 11R) were prepared as one set of fluorescent peptides, by conventional Fmoc-based solid-phase peptide synthesis as described previously [17].

2.2. Construction of poly-arginine-eGFP and -p53 vectors

We constructed bacterial expression vectors to produce the poly-arginine fusion proteins. Each vector was constructed by modification of the vector pET-21a(+) (Novagen, Madison, WI) as described previously [14]. Briefly, the vectors were tagged with a 6-histidine leader followed by each poly-arginine (3R, 5R, 7R, 9R and 11R) flanked by glycine and glutamic acid residues (for free bond rotation of the domain) in the C-terminus. The eGFP and human wild-type p53 cDNAs were subcloned into NotI/XhoI and HindIII/XhoI sites of the vectors, respectively, as described in our previous paper [11,13].

2.3. Expression and purification of recombinant proteins

Each recombinant protein (p53, p53-3R, p53-7R and p53-11R) was generated as described previously [13]. Briefly, the constructed plasmids were transformed into BL21-DE3 *Escherichia coli* cells. The proteins were expressed in these cells after induction with 0.1 mM isopropyl-1-thio-ß-D-galactopyranoside. The expressed proteins were purified using a column of Ni-NTA agarose (Invitrogen, San Diego, CA). After dialysis against PBS, the proteins were stored at −80 °C. The cells transformed with eGFP were incubated for overnight at 25 °C, and p53-PTD was incubated for 4 h at 37 °C prior to use.

Cells were harvested and resuspended in 30 ml of lysis buffer containing 20 mM HEPES, pH8.0, 100 mM NaCl and 8 M urea. They were then sonicated and the supernatant was recovered and applied to a column of Ni. The column was washed 3 times with washing buffer (20 mM HEPES, pH8.0, 100 mM NaCl, 8 M urea, and 40 mM imidazol) and eluted by elution buffer (20 mM HEPES, pH8.0, 100 mM NaCl, 8 M urea, and 40 mM imidazol). The eluted protein was dialyzed by PBS buffer with a dialysis cassette (#66810, Thermo Scientific, IL, USA) and then concentrated by centrifugal filter devices (#4422, Millipore Corporation, MA, USA) and kept at −80 °C.

2.4. Cell lines and cell culture

U251-MG, Hela, and HEK293 cells were provided from Health Science Research Resources Bank (Osaka, Japan). LNZ308 and U87 cells were kindly provided by Prof. W. Cavenee and Dr. A. Mukasa at UCSD. Rat primary astrocytes were prepared from a newborn Wistar rat (Japan SLC Inc.). The cortex of the rat on postnatal 1 day was dissected and the meninges were removed. The cortical tissues were then treated with 0.25% trypsin (Gibco) for 15 min at 37 °C and further treated with 0.004% DNase-I (Sigma) for 10 min. The pieces of the cortex were mechanically dissociated. The dissociated cells were plated onto collagen-coated glass slides and collagen-coated 96-well dishes. The cells were maintained in Dulbecco's modified Eagle's medium (D-MEM, Gibco) with 10% fetal calf serum (Gibco) and 5% horse serum. Cultures were maintained at 37 °C in a 95% air/5% CO_2 humidified incubator.

K562 cells were maintained in RPMI Medium 1640 (Gibco) supplemented with 10% fetal bovine serum, 100 U/ml penicillin and 100 U/ml streptomycin. Primary rat fibroblasts were maintained in MEM (Wako) supplemented with 10% fetal bovine serum, 100 U/ml penicillin and 100 U/ml streptomycin.

2.5. Protein/peptide transduction into cells

The transduction of proteins and peptides into cells was carried out as described previously [18]. Briefly, cells were plated onto dishes (diameter 3 cm) and incubated in D-MEM containing 10% FBS (Thermo Fisher Scientific), and 1% penicillin and streptomycin for 48 h in a humidified atmosphere containing 5% CO_2. After removal of the medium, the cells were washed twice with PBS and incubated with 50 μM 1-pyrenebutyric acid (PB, Sigma–Aldrich) in PBS for 2 min at 37 °C, and then each protein or peptide dissolved in PBS was added. After 20 min, the cells were washed two times with PBS and further incubated in new medium for the period indicated.

2.6. Confocal laser microscopic analysis

Cells (2×10^5) were plated onto 35 mm-diameter glass-bottomed dishes (Iwaki) coated with laminin and cultured for 48 h. After the transduction of poly-arginine-fused eGFP, the cells were washed twice with PBS and the medium was replaced with D-MEM containing 10% (v/v) calf serum, and 1% penicillin and streptomycin. The GFP and TMR signals were observed in living cells using a confocal laser microscope (FV300, Olympus, Tokyo) equipped with a 60× objective lens.

2.7. Western blot analysis

Western blotting was carried out at high stringency, essentially as described previously [19]. The harvested cells were lysed by a sonicator in a boiled buffer containing 1% SDS. The cell lysate (50 μg) was subjected to SDS-PAGE and transferred to nitrocellulose membranes (Hybond ECL, Amersham Biosciences). The blots were probed with primary antibodies against p53 (1:400) (*Pab 1801, Santa Cruz Biotechnology, Inc., Santa Cruz, CA*) and eGFP. Specific bands were visualized with an enhanced chemiluminescence detection kit (Amersham Biosciences). For detection of the ubiqutination of 3R-p53 proteins, U251-MG cells were transduced with 1 μM of the p53-3R protein and pyrenbutyrate for 8 h in the presence or absence of 25 μM MG132, a proteasome inhibitor. The cells were then collected and homogenized in SDS-PAGE buffer. Whole-cell extracts (100 μg of protein) were analyzed by Western blotting with anti-p53 antibody (Pab 1801; Santa Cruz Biotechnology).

2.8. Reporter assay for p21/waf1 luciferase-driven p53 transactivation

The reporter assay was performed as described [14]. The luciferase reporter vector containing a 2.4 kbp fragment of the human p21/WAF1 promoter was a gift from Drs. T. Akiyama (Tokyo University) and K. Yoshikawa (Osaka University). LNG308 cells grown until 80% confluent in 35 mm-diameter dishes were transfected with the luciferase reporter vector by the calcium phosphate method. After 24 h, the cells were incubated with 500 nM of p53-11R, -7R, and -3R in PBS for 20 min and further cultured in new medium. Cells were harvested 2 and 24 h after the protein transduction and the cell lysate was used for measuring luciferase activity with a luminometer and a reagent kit (Tokyo Ink, Tokyo, Japan). The background luciferase activity was subtracted in all experiments.

2.9. Cell viability assay (WST-1 assay)

Cell viability was determined using the WST-1 (2-[2-methoxy-4-nitrophenyl]-3-[4-nitrophenyl]-5-[2,4-disulfophenyl]-2H-tetrazolium, mono sodium salt) assay (Roche Applied Science) as described previously [19]. After protein transduction, U251-MG cells (1×10^3 per well) seeded onto 96-well plates were cultured in D-MEM containing 10% fetal bovine serum, and 1% penicillin and streptomycin for 24 h. After being washed with PBS, the cells were placed in fresh D-MEM and incubated for 96 h. Cell viability was measured using the WST-1 assay on Day 4 according to the manufacturer's instructions (Roche Applied Science).

2.10. Semi quantification of intracellular TM- fused peptide

U251-MG cells (5×10^4/well) were incubated with 10 μM TMR-3R, TMR-5R, TMR-7R, TMR-9R and TMR-11R in D-MEM containing 10% BSA and 5% penicillin/streptomycin for 0.5 h or 4 h at 37 °C. The cells were washed twice with PBS, and 0.2 ml of 1% SDS was added. After homogenization, the cell lysate was subjected to analysis. Intracellular TMR content was measured by fluorescence spectrophotometer (FP-6600, Japan Spectroscopic Corporation, Japan) at an excitation wavelength of 550 nm and an emission wavelength of 580 nm.

2.11. Statistical analysis

Data are shown as the mean ± S.E.M. Data were analyzed using either Student's *t*-test to compare two conditions or ANOVA followed by planned comparisons of multiple conditions, and $P < 0.05$ was considered to be significant.

3. Results

3.1. Comparison of the efficiency of transduction of each poly-arginine peptide in glioma cells

U251-MG cells, a human glioma cell line, were transduced with 1 μM of 3R, 5R, 7R, 9R, or 11R peptide fused with TMR, a red fluorescence protein, with or without pyrenebutyrate, and transduction efficiency was compared. TMR signals were observed after 0.5 h in the cells transduced with each peptide irrespective of treatment with pyrenebutyrate, and the strength of the signals was the same as that 4 h after the transduction, suggesting that the

poly-arginine peptides were rapidly transduced into the cells (Fig. 1A). However, without pyrenebutyrate, the efficiency of the transduction differed among the peptides and depended on the number of arginine residues (Fig. 1A). 3R-TMR was observed in a few cells without pyrenebutyrate (Fig. 1A). In contrast, pyrenebutyrate induced the transduction. 7R-, 9R- and 11R-TMR were delivered into all cells and 3R-TMR was observed in more than 60% of cells treated with pyrenebutyrate (Fig. 1A). Moreover, poly-arginine peptides delivered without pyrenebutyrate accumulated in the organelles whereas the peptides transduced with pyrenebutyrate spread into the cytoplasm and nucleus 0.5 h after the transduction (Fig. 1A).

3.2. Transduction of 3R- and 11R-TMR with pyrenebutyrate at 4 °C

Poly-arginine peptides are delivered into cells via physiological mechanisms such as macropinocytosis [20–22]. Therefore, a considerable decrease in the cellular uptake of peptides is observed when the cells are treated at 4 °C [18]. In contrast, a previous study showed that the addition of pyrenebutyrate resulted in the direct membrane translocation of 8R [18]. To investigate whether 3R-TMR can also be artificially delivered into cells with pyrenebutyrate, U251-MG cells were incubated with 3R- and 11R-TMR at 4 °C. Faint signals for both 3R- and 11R-TMR were observed in a few cells without pyrenebutyrate (Fig. 1B). In contrast, strong signals for 3R- and 11R-TMR were observed in the cells co-treated with pyrenebutyrate (Fig. 1B). 11R-TMR was delivered to all cells and 3R-TMR was transduced into about 40% of cells with pyrenebutyrate at 4 °C (Fig. 1B). These results suggest that 3R-TMR was artificially delivered to glioma cells with pyrenebutyrate.

3.3. Semi-quantitative analysis of transduced peptide in U251 cells by fluorescence spectrophotometer

To compare the amount of intracellular uptake of each peptide, fluorescence of TMR was measured with the spectrophotometer at an excitation wavelength of 550 nm and an emission wavelength of 580 nm. After 0.5 h, the intracellular uptake of 5R-, 7R-, and 9R-TMR peptides with pyrenebutyrate was almost twice that without pyrenebutyrate (Fig. 1C). However, the uptake of 3R-TMR with pyrenebutyrate was about 5-fold that without pyrenebutyrate (Fig. 1C). The intracellular uptake of 11R-TMR peptide with pyrenebutyrate increased 20% compared to that without pyrenebutyrate. These results suggest that pyrenebutyrate is most effective for the transduction of 3R-TMR.

3.4. Effect of 3R fusion on protein transduction in cells

We next examined whether 3R has the ability to transduce protein in tumor cells. U251-MG cells were incubated with eGFP-3R in the presence or absence of pyrenebutyrate, and the efficiency of the transduction was examined in living cells. The eGFP-3R was detected on the cell membrane at 0.5 h and in the perinuclear cytoplasm at 2 h post–transduction, with or without pyrenebutyrate (Fig. 2A). After 4 and 8 h, the eGFP-3R signal was faint in the absence of pyrenebutyrate (Fig. 2A). In contrast, a strong signal for eGFP-3R was observed in the perinuclear cytoplasm and nucleus in the presence of pyrenebutyrate 4 and 8 h after the transduction (Fig. 2A). To investigate whether eGFP-3R was delivered into various cell types in the presence of pyrenebutyrate, we examined its transduction in primary cultured cells [rat astrocytes (Fig. 2B-i) and mouse fibroblasts (Fig. 2B-j)], cancer cells [H520 (Fig. 2B-k), U87MG (Fig. 2B-l) and LNZ308 (Fig. 2B-m)] and floating cells [K562 (Fig. 2B-n)]. Cellular uptake of eGFP-3R was observed in all cell types (Fig. 2B). However, the subcellular distribution of eGFP-3R differed among the types. The protein was observed in both the cytosol and nucleus in primary cultured cells and H520 cells, in the perinuclear cytoplasm in U87MG and LNZ308 cells and in the nucleus in K562 cells (Fig. 2B).

3.5. Cellular uptake of p53-3R in glioma cells

We previously showed that p53-11R and p53-9R were delivered into cancer cells and exhibited transcriptional activity without pyrenebutyrate [13]. We next examined whether p53-3R was delivered to U251-MG cells and the effect of pyrenebutyrate on the transduction in the cells. Interestingly, p53-3R was delivered regardless of pyrenebutyrate (Fig. 3A). However, the subcellular distribution of p53-3R differed in the presence and absence of pyrenebutyrate. With pyrenebutyrate, p53-3R was mainly observed in the nucleus whereas without pyrenebutyrate, it existed in the cytoplasm of U251-MG cells (Fig. 3A). Next the effect of pyrenebutyrate on the time-dependent transduction of 3R-p53 in the glioma cells was examined. Contrary to the results for eGFP-3R in Fig. 1, more p53-3R was transduced without than with pyrenebutyrate 0.5, 2 and 8 h after the transduction (Fig. 3B). We also examined the effect of pyrenebutyrate on p53-11R transduction. More p53-11R was also transduced without the chemical (Fig. 3C).

The wild-type p53 protein is rapidly degraded by the ubiquitin-proteasome system [23,24]. Moreover, we previously showed that p53-11R was rapidly degraded by the ubiquitin-proteasome [19]. Therefore, we speculated that p53-3R was degraded more rapidly with than without pyrenebutyrate by the ubiquitin-proteasome system. We next examined whether MG132, a proteasome inhibitor, inhibited the degradation of p53-3R. With pyrenebutyrate in the presence of MG132, p53-3R was highly ubiquitinated by the ubiquitin-proteasome pathway (Fig. 3D).

3.6. Comparison of p53 transcriptional activity among p53-3R, p53-7R and p53-11R with or without pyrenebutyrate

To compare the transcriptional activity among p53-3R, p53-7R, and p53-11R in glioma cells, each protein (1 μM) was transduced into LNZ308 cells lacking the p53 gene, and time-dependent p53 transcriptional activity was examined. In the absence of pyrenebutyrate, all of the poly-arginine-fused p53 proteins showed low transcriptional activity (Figs. 4A and 2h with pyrenebutyrate; control, 1533.5 ± 124.3, p53-3R, 24931 ± 100.5, p53-7R, 22318 ± 211.3, p53-11R, 19721 ± 911.1; 2 h without Pyrenebutyrate : control, 1533.5 ± 124.3, p53-3R, 6220.3 ± 167.2, p53-7R, 5714 ± 38.1, p53-11R, 11491 ± 331.4; 24 h with Pyrenebutyrate; control, 1533.5 ± 124.2, p53-3R, 34256.8 ± 3913.3, p53-7R, 29132.8 ± 2524.4, p53-11R, 27391.8 ± 1057.5; 24 h without Pyrenebutyrate : control, 1533.5 ± 124.2, p53-3R, 16352.8 ± 589.2, p53-7R, 15517.3 ± 3726.8, p53-11R, 12234.3 ± 788.8; $n = 6$ each, $^*P < 0.01$). However, in the presence of pyrenebutyrate, the transcriptional activity in p53-3R-transduced cells was significantly higher than that in the p53-7R and 11R-transduced cells both 2 and 24 h after the transduction of each protein (Fig. 4A).

3.7. Inhibition of cell proliferation by p53-3R with pyrenebutyrate against glioma cells

Finally, we examined whether p53-3R inhibited the growth of cancer cells with pyrenebutyrate. U251-MG cells were treated with 1 and 10 μM of p53-3R, p53-11R or p53 without CPP. In the absence of pyrenebutyrate, a single application of p53-3R, p53-11R and p53 could not inhibit the growth of U251-MG cells (Fig. 4B). Moreover, neither 1 nor 10 μM of p53-11R affected cell growth even in the presence of pyrenebutyrate. In contrast, a single application of 10 or

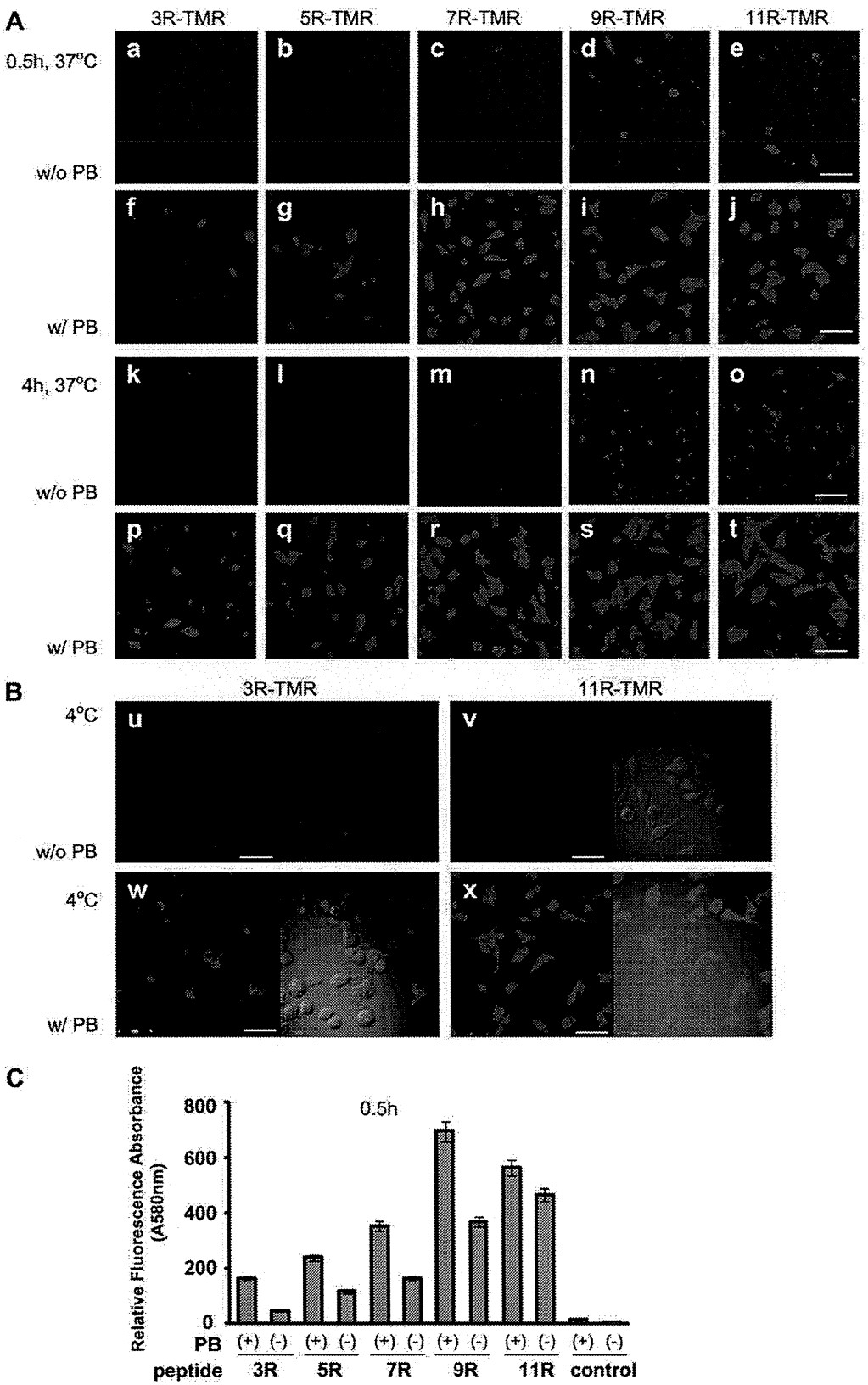

Fig. 1. Comparison of the efficiency of the delivery of 3R, 5R, 7R, 9R and 11R with or without pyrenebutyrate in U251-MG cells. (A) Time-dependent changes (0.5 h (a–j) and 4 h (k–t)) in the transduction of each poly-arginine peptide (3R, 5R, 7R, 9R, and 11R) at 37 °C with (f-j, p-t) or without pyrenebutyrate (a-e, k-o) under a confocal microscope. Bars = 10 μm. (B) The distribution of 3R-TMR (u, w) and 11R-TMR (v, x) with or without pyrenebutyrate at 4 °C. Bars = 10 μm. (C) Comparison of intracellular peptide (3R-, 5R-, 7R-, 9R- and 11R-TMR) uptake 0.5 h after the transduction with or without pyrenebutyrate.

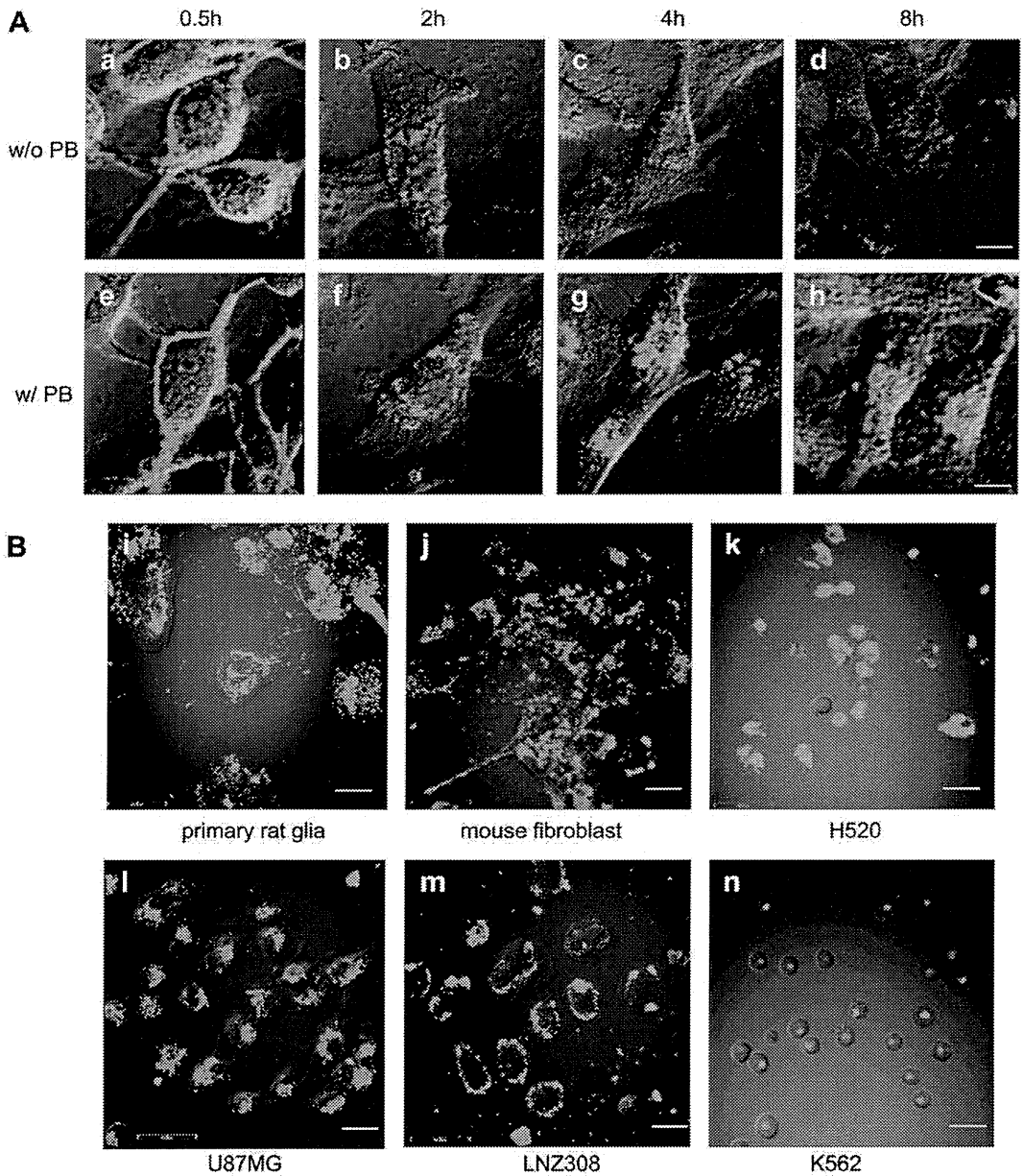

Fig. 2. Protein transduction of eGFP-3R in various cell types. (A) Comparison of time-dependent subcellular localization of transduced eGFR-3R with or without pyrenebutyrate in U251-MG cells. Bars = 10 μm. (B) Protein transduction of eGFR-3R with pyrenebutyrate in primary rat glial cells (i), mouse primary fibroblasts (j), H520 cells (k), U87MG cells (l), LNZ308 cells (m) and K562 cells (n). The cells were incubated with eGFP-3R for 4 h and the GFP signals were then observed under a confocal microscope. Bars = 10 μm.

1 μM of p53-3R significantly inhibited the growth of the glioma cells with pyrenebutyrate (Fig. 4B). These results showed that only p53-3R with pyrenebutyrate significantly inhibited the growth of U251-MG glioma cells. To investigate the toxicity of pyrenebutyrate, the cells were treated with pyrenebutyrate. However, the chemical had no effect on growth (PB only in Fig. 4B).

4. Discussion

Protein transduction using CPPs such as poly-arginine peptides (9R and 11R) and the TAT PTD is useful for delivering materials into cells *in vitro* and *in vivo* [9,10,25]. The mechanism of transduction with CPPs is thought to be rapid internalization by lipid raft-dependent macropinocytosis [26]. However, most of the internalized protein is entrapped in macropinosomes and does not function in cells [26]. Indeed, the present results showed that poly-arginine peptides occurred in the cytoplasm of cells (Fig. 1A). In contrast, poly-arginine peptides of various lengths (3R–11R) rapidly spread into the cytoplasm when co-applied with pyrenebutyrate. This result is consistent with a previous finding that a poly-arginine (8R)-fused protein directly crossed the cell membrane but not through macropinocytosis when co-applied with pyrenebutyrate [18,27]. Moreover, the transcriptional activity of 3R-p53 was higher with than without pyrenebutyrate. These results suggest that pyrenebutyrate increases levels of functional poly-arginine-fused proteins by preventing trapping in the macropinosomes and

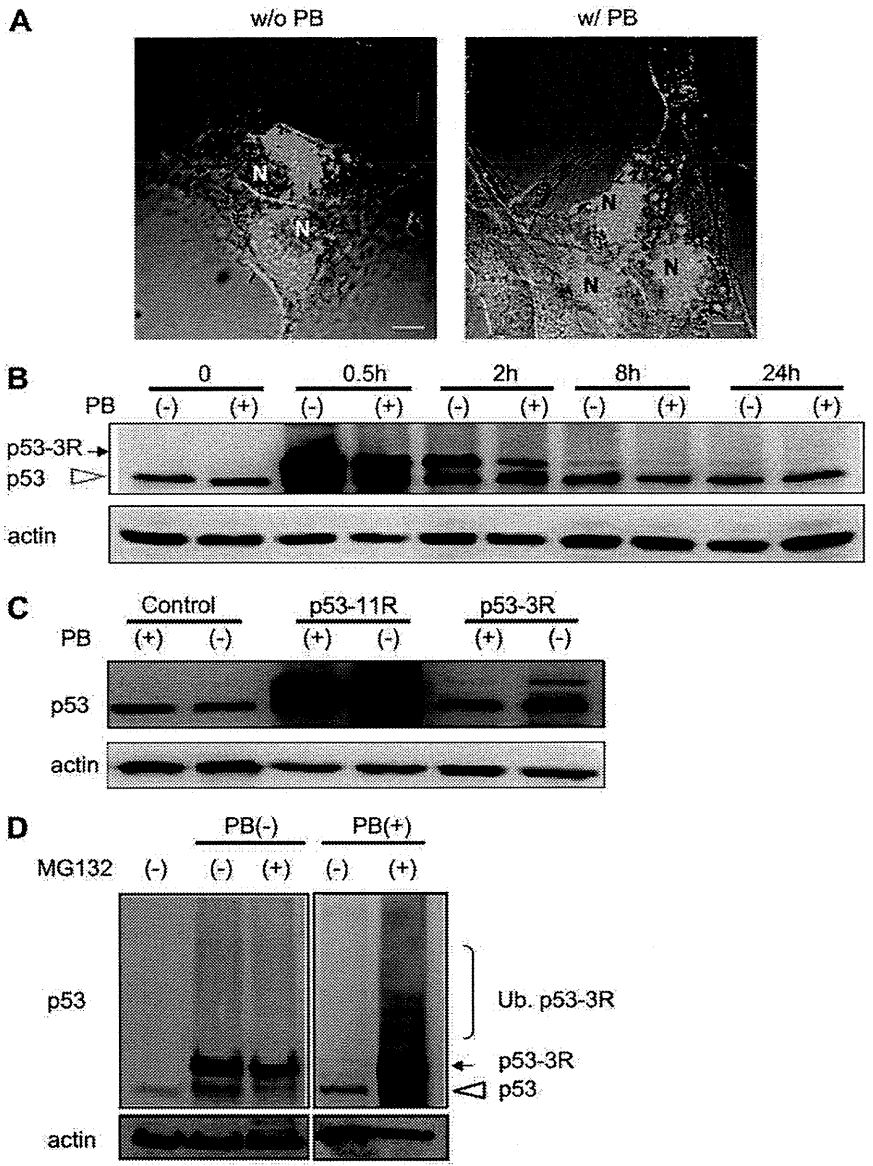

Fig. 3. Intracellular distribution and time-dependent transduction of p53-3R with or without pyrenebutyrate. (A) Confocal micrographs of p53-3R-fused with FITC in U251-MG glioma cells with or without pyrenebutyrate 4 h after the transduction. N, nucleus. Bars = 2.5 μm. (B) Time-dependent changes in the amount of transduced p53-3R with or without pyrenebutyrate in U251 glioma cells at 0, 0.5, 2, 8, and 24 h. Arrow, p53-3R protein; Arrowhead, endogenous mutated p53 protein. (C) Comparison of the amounts of p53-11R and p53-3R proteins in U251-MG cells with or without pyrenebutyrate 8 h after the transduction. (D) Comparison of intracellular transduced p53-3R protein with or without pyrenebutyrate in the presence or absence of the proteasome inhibitor MG132 for 8 h in U251-MG cells.

is useful for protein transduction using oligo-arginine peptides such as 3R.

Pyrenebutyrate is sometimes mistaken for benzopyrene, which is found in coal tar and shows evidence of carcinogenicity in lung cells [28]. However, the two have very different chemical properties. Pyrenebutyrate (1-pyrenebutyrate) is a pyrene, a polycyclic aromatic hydrocarbon consisting of four fused benzene rings, and contains a hydrophilic carboxylic acid. By contrast, benzopyrene has five benzene rings and no hydrophilic carboxylic acid. Pyrenebutyrate is easily dissolved in water, whereas benzopyrene is not. Benzopyrene, however, is highly carcinogenic. Pyrenebutyrate is not particularly toxic, though it can cause skin irritation. Pyrenebutyrate's lack of toxicity was confirmed by the results of both this study and previous reports [29].

The efficiency of protein/peptide transduction by poly-arginine peptides without pyrenebutyrate depends on the number of arginine residues [30]. However, an increase in this number may influence the functions of the fused proteins because of non-physiological interactions of the arginine with negatively charged DNA and acidic amino acids. Indeed some recombinant forms of transcription factors fused with poly-arginine do not function even when delivered into cells [13]. Reducing the number of fused arginine residues may overcome this problem. However, a decrease in the number of arginines reduces the efficiency of transduction. In the present study, we developed a new protein transduction system using an oligo-arginine (3R) and pyrenebutyrate. P53-3R had higher transcriptional activity and more markedly inhibited the growth of cancer cells than p53-11R when co-applied with

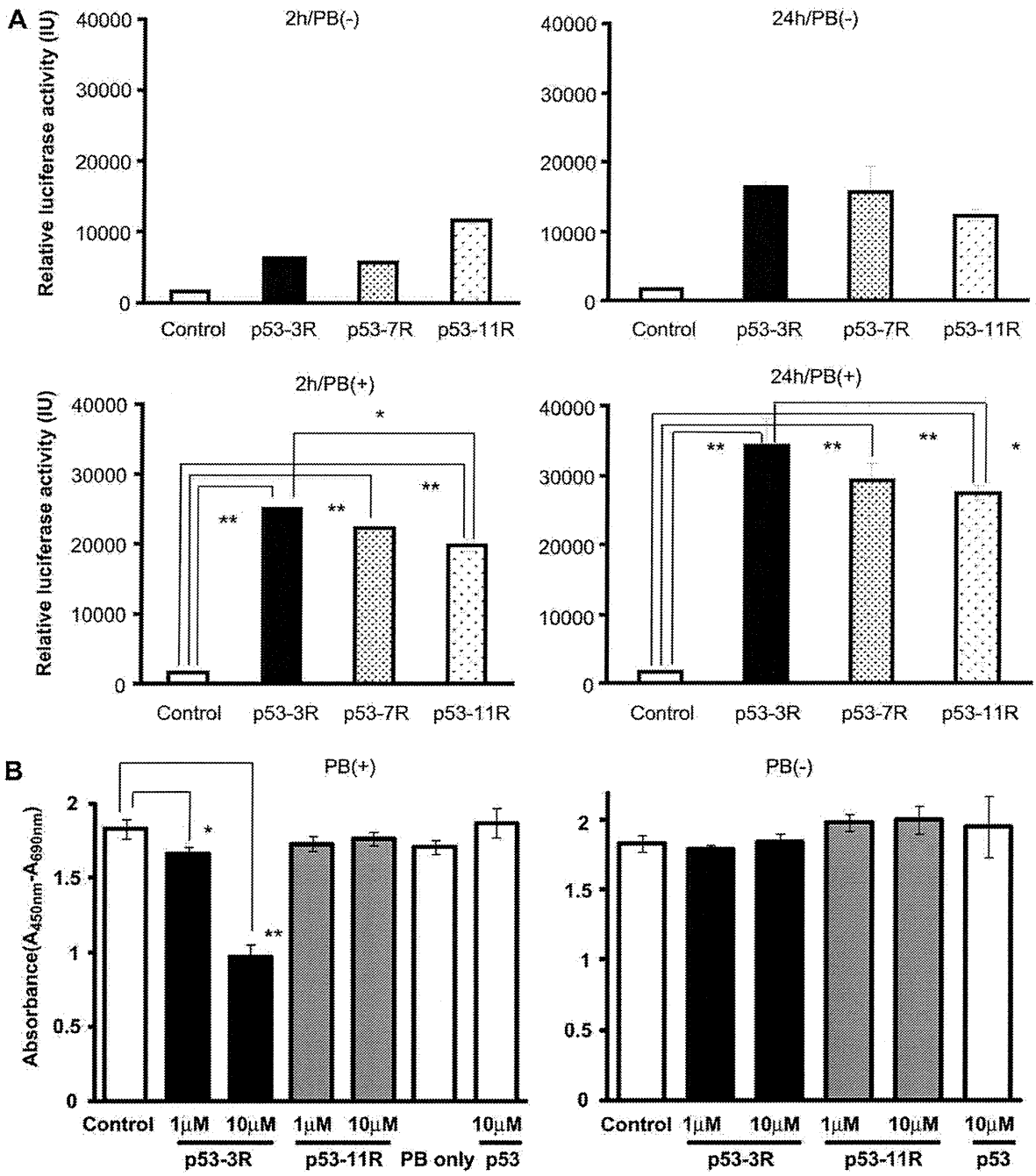

Fig. 4. Assay of p53 transcriptional activity and inhibitory effects on the proliferation of glioma cells by p53-3R, p53-7R, or p53-11R transduction with or without pyrenebutyrate. (A) p53-driven transcriptional activity with the p21/waf1 luciferace reporter assay. Upper left, 2 h without pyrenebutyrate; upper right, 24 h without pyrenebutyrate; lower left, 2 h with pyrenebutyrate; lower right, 24 h with pyrenebutyrate. Cont, no protein transduction. Data are presented as the mean ± S.E.M. $n = 6$ in each group. $^{*}P < 0.01$, $^{**}P < 0.001$. (B) Inhibitory effect of each protein on glioma cell proliferation. Cell viability was measured by the WST-1 assay on Day 4. Left, with pyrenebutyrate; right, without pyrenebutyrate. Cont, no protein transduction. Data are presented as the mean ± S.E.M. n = 6 in each group. $^{*}P < 0.05$, $^{**}P < 0.01$.

pyrenebutyrate, even though the amount transduced was one-eighth that of p53-11R. Transcription factors bind to promoters of DNA and start transcription. The fusion of 3R may reduce the extent to which the activity of the fused transcription factors is disrupted. Furthermore, in a bacterial protein expression system, the expression of poly-arginine-fused proteins is smaller than that of proteins not fused to arginine domains. A shorter arginine domain-fused protein is more easily purified from such a system. This is a major advantage of protein transduction for making a cell membrane-permeable peptide-fused protein.

5. Conclusion

The present results showed that an oligo-arginine (3R) was effective at delivering a transcription factor with activity into the nucleus of cells. It appears that our system can be used to deliver

transcription factors into various cells. Protein transduction using 3R with pyrenebutyrate may overcome the disadvantages of previous methods and become a promising modality for cancer therapy.

Acknowledgments

We thank A. Ueda for technical assistance, T. Akiyama and K. Yoshikawa for the luciferase reporter vector for the p21/WAF1 promoter, and A. Mukasa and W. Cavenee for U87MG and LNZ308 cells. This work was supported by a Grant-in-aid for Scientific Research from the Ministry of Education, Science, Sports and Culture of Japan and by a Grant-in-aid for Scientific Research from the Ministry of Health, Labor and Welfare of Japan.

References

[1] Prochiantz A. Messenger proteins: homeoproteins, TAT and others. Curr Opin Cell Biol 2000;12:400–6.
[2] Vives E. Cellular uptake [correction of utake] of the Tat peptide: an endocytosis mechanism following ionic interactions. J Mol Recognit 2003;16:265–71.
[3] Schwarze SR, Ho A, Vocero-Akbani A, Dowdy SF. In vivo protein transduction: delivery of a biologically active protein into the mouse. Science 1999; 285(5433):1569–72.
[4] Wadia JS, Dowdy SF. Protein transduction technology. Curr Opin Biotechnol 2002;13(1):52–6.
[5] Eguchi A, Meade BR, Chang YC, Fredrickson CT, Willert K, Puri N. Efficient siRNA delivery into primary cells by a peptide transduction domain-dsRNA binding domain fusion protein. Nat Biotechnol 2009;27(6):567–71.
[6] Michiue H, Eguchi A, Scadeng M, Dowdy SF. Induction of in vivo synthetic lethal RNAi responses to treat glioblastoma. Cancer Biol Ther 2009;23: 2306–13.
[7] Vivès E, Brodin P, Lebleu B. A truncated HIV-1 Tat protein basic domain rapidly translocates through the plasma membrane and accumulates in the cell nucleus. J Biol Chem 1997;272(25):16010–7.
[8] Suzuki T, Futaki S, Niwa M, Tanaka S, Ueda K, Sugiur Y. Possible existence of common internalization mechanisms among arginine-rich peptides. J Biol Chem 2002;277(4):2437–43.
[9] Matsui H, Tomizawa K, Lu YF, Matsushita M. Protein therapy: in vivo protein transduction by polyarginine (11R) PTD and subcellular targeting delivery. Curr Protein Pept Sci 2003;4:151–7.
[10] Futaki S, Ohashi W, Suzuki T, Niwa M, Tanaka S, Ueda K. Stearylated arginine-rich peptides: a new class of transfection systems. Bioconjug Chem 2001; 12(6):1005–11.
[11] Matsushita M, Tomizawa K, Moriwaki M, Li SH, Terada H, Ohmoto T. A high-efficiency protein transduction system demonstrating the role of PKA in long-lasting long-term potentiation. J Neurosci 2001;21:6000–7.
[12] Tomizawa K, Sunada S, Lu YF, Oda Y, Kinuta M, Ohshima T. Cophosphorylation of amphiphysin I and dynamin I by Cdk5 regulates clathrin-mediated endocytosis of synaptic vesicles. J Cell Biol 2003;163(4):813–24.
[13] Michiue H, Tomizawa K, Wei FY, Matsushita M, Lu YF, Ichikawa T. The NH2 terminus of influenza virus hemagglutinin-2 subunit peptides enhances the antitumor potency of polyarginine-mediated p53 protein transduction. J Biol Chem. 2005;280(9):8285–9.
[14] Takenobu T, Tomizawa K, Matsushita M, Li ST, Moriwaki A, Lu YF. Development of p53 protein transduction therapy using membrane-permeable peptides and the application to oral cancer cells. Mol Cancer Ther 2002;12:1043–9.
[15] Ozaki T, Nakagawara A. p53: the attractive tumor suppressor in the cancer research field. J Biomed Biotechnol 2011;2011:603925.
[16] Datto MB, Yu Y, Wang XF. Functional analysis of the transforming growth factor beta responsive elements in the WAF1/Cip1/p21 promoter. J Biol Chem 1995;270(48):28623–8.
[17] Kitamatsu M, Kashiwagi T, Sisido M. Synthesis of a newly peptide nucleic acid that contains tertiary amino groups. Nucleic Acids Symp Ser (Oxf) 2005;(49):363–4.
[18] Takeuchi T, Kosuge M, Tadokoro A, Sugiura Y, Nishi M, Kawata M. Cellular internalization and distribution of arginine-rich peptides as a function of extracellular peptide concentration, serum, and plasma membrane associated proteoglycans. Bioconjug Chem 2008;19(3):656–64.
[19] Michiue H, Tomizawa K, Matsushita M, Tamiya T, Lu YF, Ichikawa T. Ubiquitination-resistant p53 protein transduction therapy facilitates anti-cancer effect on the growth of human malignant glioma cells. FEBS Lett 2005; 579(18):3965–9.
[20] Wadia JS, Stan RV, Dowdy SF. Transducible TAT-HA fusogenic peptide enhances escape of TAT-fusion proteins after lipid raft macropinocytosis. Nat Med 2004;10(3):310–5.
[21] Matsushita M, Noguchi H, Lu YF, Tomizawa K, Michiue H, Li ST. Photo-acceleration of protein release from endosome in the protein transduction system. FEBS Lett 2004;572(1–3):221–6.
[22] Wadia JS, Dowdy SF. Transmembrane delivery of protein and peptide drugs by TAT-mediated transduction in the treatment of cancer. Adv Drug Deliv Rev 2005;57(4):579–96.
[23] Michael D, Oren M. The p53-Mdm2 module and the ubiquitin system. Semin Cancer Biol 2003;13(1):49–58.
[24] Rodriguez MS, Desterro JM, Lain S, Lane DP, Hay RT. Multiple C-terminal lysine residues target p53 for ubiquitin-proteasome-mediated degradation. Mol Cell Biol 2000;20(22):8458–67.
[25] Fittipaldi A, Giacca M. Transcellular protein transduction using the Tat protein of HIV-1. Adv Drug Deliv Rev 2005;57(4):597–608.
[26] Jablonski AE, Kawakami T, Ting AY, Payne CK. Pyrenebutyrate leads to cellular binding, not intracellular delivery, of polyarginine-quantum dots. J Phys Chem Lett 2010;1:1312–5.
[27] June RK, Gogoi K, Eguchi A, Cui XS, Dowdy SF. Synthesis of a pH-sensitive nitrilotriacetic linker to peptide transduction domains to enable intracellular delivery of histidine imidazole ring-containing macromolecules. J Am Chem Soc 2010;132(31):10680–2.
[28] Panwar M, Samarth R, Kumar M, Yoon WJ, Kumar A. Inhibition of benzo(a) pyrene induced lung adenoma by panax ginseng extract, EFLA400, in Swiss albino mice. Biol Pharm Bull 2005;(11):2063–7.
[29] Guterstam P, Madani F, Hirose H, Takeuchi T, Futaki S, El Andaloussi S. Elucidating cell-penetrating peptide mechanisms of action for membrane interaction, cellular uptake, and translocation utilizing the hydrophobic counter-anion pyrenebutyrate. Biochim Biophys Acta 2009;1788(12):2509–17.
[30] Matsushita M, Tomizawa K, Moriwaki A, Li ST, Terada H, Matsui H. A high-efficiency protein transduction system demonstrating the role of PKA in long-lasting long-term potentiation. J Neurosci 2001;21(16):6000–7.

Neuroscience 200 (2012) 13–18

ANTIDEPRESSANT-LIKE EFFECT OF SILDENAFIL THROUGH OXYTOCIN-DEPENDENT CYCLIC AMP RESPONSE ELEMENT-BINDING PROTEIN PHOSPHORYLATION

H. MATSUSHITA,[a] M. MATSUZAKI,[a] X.-J. HAN,[a] T.-I. NISHIKI,[a] I. OHMORI,[a] H. MICHIUE,[a] H. MATSUI[a] AND K. TOMIZAWA[b]*

[a]*Department of Physiology, Okayama University Graduate School of Medicine, Dentistry and Pharmaceutical Sciences, Okayama 700-8558, Japan*

[b]*Department of Molecular Physiology, Faculty of Life Sciences, Kumamoto University, Kumamoto 860-8556, Japan*

Abstract—Oxytocin (OT) levels in plasma increase during sexual response and are significantly lower in patients with depression. A drug for the treatment of sexual dysfunction, sildenafil, enhances the electrically evoked release of OT from the posterior pituitary. In this study, we showed that sildenafil had an antidepressant-like effect through activation of an OT signaling pathway. Application of sildenafil reduced depression-related behavior in male mice. The antidepressant-like effect was blocked by an OT receptor (OTR) antagonist and was absent in OTR knockout (KO) mice. Sildenafil increased the phosphorylation of cAMP response element-binding protein (CREB) in the hippocampus. The OTR antagonist inhibited sildenafil-induced CREB phosphorylation and sildenafil had no effect on CREB phosphorylation in OTR KO mice. These results suggest sildenafil to have an antidepressant-like effect through the activation of OT signaling and to be a promising drug for the treatment of depression.

Key words: oxytocin, depression, CREB, sildenafil, anxiety, MAP kinase.

Oxytocin (OT) is an acknowledged hormone for uterine contractions during labor and milk ejection during lactation in mammals (Gainer and Wray, 1994; Neumann, 2001). OT acts as a neurotransmitter/neuromodulator to regulate a diverse range of CNS functions in both males and females, including emotional (Neumann, 2008), parental (Numan and Insel, 2003), affiliative (Insel and Shapiro, 1992), and sexual (Argiolas and Gessa, 1991) behaviors, as well as spatial and social memories (Tomizawa et al., 2003; Bielsky and Young, 2004). In rats and mice, moreover, OT is known as an antidepressant effecter (Arletti and Bertolini, 1987; Ring et al., 2010; Matsushita et al., 2010). Clinical studies have attempted to correlate the level of OT circulating in plasma with depressive symptomology. Reduced plasma OT concentrations were observed in patients with major depressive disorder (MDD) compared with controls (Frasch et al., 1995; Zetzsche et al., 1996). A similar finding was recently made in a female cohort study of patients with MDD (Ozsoy et al., 2009).

Alterations to the structure and function of the hippocampus could contribute to certain aspects of MDD, including disruption of cognition, depressed mood, helplessness, anhedonia, and control of the hypothalamic-pituitary-adrenal axis (McEwen, 1999; Drevets, 2000, 2001). Increases in neurogenesis, plasticity, and neural survival through the activation of a MAP kinase cascade and subsequent enhanced phosphorylation of CREB in the hippocampus have been proposed as common mediators of antidepressant efficacy (D'Sa and Duman, 2002; Gourley et al., 2008; Duric et al., 2010). Moreover, we previously showed that OT induced the phosphorylation of cAMP response element-binding protein (CREB) through activation of MAP kinase signaling and induced neural plasticity in the hippocampus (Tomizawa et al., 2003). These results suggest a potential antidepressant-like effect and therapeutic benefit from OT through the activation of MAP kinase signaling and subsequent phosphorylation of CREB in patients with MDD. However, therapeutic use in humans has been hampered because OT does not readily pass the blood–brain barrier (BBB) when administered systemically and evokes potent hormone-like side effects when circulating in the blood. Although the intranasal administration of OT is under clinical trials, it remains to be proven safe and effective (Slattery and Neumann, 2010).

Sildenafil citrate (Viagra®; Pfizer, NY, USA) is a selective inhibitor of the cyclic guanosine monophosphate (cGMP)-specific phosphodiesterase type 5 (PDE5) enzyme and widely used to treat erectile dysfunction (Boolell et al., 1996). Recent studies have shown that sildenafil modulates functions in the CNS, especially OT signaling. For instance, sildenafil enhances the electrically evoked release of OT from the posterior pituitary through cGMP-mediated modulation of K^+ channels in the neurohypophysis (Zhang et al., 2007) and OT expression in the paraventricular nucleus (Shin et al., 2010). Moreover, sildenafil shows antidepressant-like activity (Brink et al., 2008; Liebenberg et al., 2010a,b, 2011) and induced neuroplasticity (Zhang et al., 2002, 2006a,b). These results suggest sildenafil to have an antidepressant-like effect through the induction of OT secretion and activation of a subsequent signaling cascade such as MAP kinase signaling and CREB phosphorylation. In the present study, we demonstrated the effect of sildenafil on depression-like behavior in male mice.

*Corresponding author. Tel: +81-96-373-5050; fax: +81-96-373-5052.
E-mail address: tomikt@kumamoto-u.ac.jp (K. Tomizawa).

Abbreviations: CREB, cAMP response element-binding protein; cGMP, cyclic guanosine monophosphate; FST, forced swim test; KO, knockout; MDD, major depressive disorder; NO, nitric oxide; OTR, Oxytocin receptor; WT, Wild-type.

0306-4522/12 $36.00
doi:10.1016/j.neuroscience.2011.11.001

MATERIALS AND METHODS

Animals

OT receptor (OTR) knockout (KO) mice were purchased from Deltagen (San Mateo, CA, USA) (Matsushita et al., 2010). Originally an equal mix of the C57BL/6 and 129X1/SvJ strains (RW4 embryonic stem cell line), they have been repetitively backcrossed for four generations with C57BL/6 mice (from Deltagen). Wild-type (WT) and OTR KO male mice (10–13 weeks old) were used for all experiments. For the mating behavior test, C57BL/6 females (12–14 weeks old) were used. The WT males used were littermates. The animals were housed in groups of 3–4. Single-housed males were individually housed for 2 weeks before testing. Animals were housed at 25 °C with 12-h light/dark cycles with free access to water and standard rodent chow in the Department of Animal Resources of Okayama University. All procedures were approved by the Animal Ethics Committee of Okayama University (OKU-2010164). All possible efforts were made to minimize the number of animals used and their suffering.

Drug application

Sildenafil, a selective inhibitor of PDE5, was purchased from Tocris Bioscience (Ellisville, MO, USA). Atosiban, an OTR antagonist, and PD184161, a MEK inhibitor, were purchased from Sigma-Aldrich (St. Louis, MO, USA). Sildenafil and atosiban were suspended in phosphate-buffered saline (PBS) before use. PD184161 was dissolved in DMSO. WT males were intraperitoneally administered with vehicle, each concentration (10, 20, 30, and 60 mg/kg) of sildenafil, 80 mg/kg of atosiban (Sigma-Aldrich), and 30 mg/kg of PD184161. Mice were injected with each drug 1 h before the forced swim test (FST).

For the successive treatments with sildenafil, mice were intraperitoneally injected with 20 mg/kg of sildenafil every 24 h for 3 days. Mice were given the FST 1 h after the final administration.

Forced swim test

Depression-like behavior was tested with the FST as described previously (Matsushita et al., 2010). Briefly, mice were placed in a glass cylinder (diameter 15 cm, height 20 cm) filled 12 cm with water kept at 24–25 °C and then made to swim once for 6 min the day before the FST as preconditioning. After 24 h, the mice were injected with each drug and vehicle and 1 h later, forced to swim for 6 min. The time spent immobile between min 3 and 6 was scored. The FST was monitored in the light phase with a video monitoring system (Actimetrics Inc., USA).

Open-field test

Total locomotor activity was tested by the open-field test as described (Fagioli et al., 1991; Weisstaub et al., 2006). Briefly, the apparatus was a square area (49×49×35 cm^3; 30 lx). Single-housed males were intraperitoneally administered with each drug 1 h before the test by a trained observer blind to the treatment. The mice were placed into the center of the open-field, and total locomotor activity was recorded for 5 min with a video/computer system (Actimetrics Inc., USA).

Mating behavior test

Male mice were administered with vehicle or 60 mg/kg of sildenafil 1 h before the mating behavior test. A male was placed with a female for 1 h in the light phase (16–35 lx), and mating behavior was confirmed based on observations of mounting via a video monitoring system (Actimetrics Inc., USA). The number of mounts was counted.

Western blotting

Western blotting was carried out at high stringency, essentially as described previously (Tomizawa et al., 2003). Briefly, the hippocampi of mice were dissected 30 min after the administration of each drug. The homogenates of hippocampus were prepared by sonicating in boiled 1% SDS buffer. The homogenates were separated by electrophoresis through a 12% SDS-PAGE gel before being transferred to a nitrocellulose membrane (Amersham Biosciences, Piscataway, NJ, USA). Blots were probed with primary antibodies against phospho-CREB (anti–phospho-CREB, Upstate, Lake Placid, NY, USA) and total CREB (anti-CREB NT, Upstate Biotechnology). After incubation with the appropriate secondary antibody conjugated with horseradish peroxidase (Sigma-Aldrich), positive bands were visualized using an enhanced chemiluminescence detection system (Amersham Biosciences, Pittsburgh, PA, USA).

Statistics

Data are shown as the mean±SEM. Student's *t*-test or Mann–Whitney's U-test was used to identify significant differences between two conditions and a one-way ANOVA or a two-way ANOVA followed by Tukey–Kramer's post hoc analysis was used to compare multiple conditions. *P* values less than 0.05 were considered to be significant.

RESULTS

Antidepressant-like effect of sildenafil in male mice

The effect of sildenafil on depression-related behavior was first examined in WT male mice. Mice were administered with vehicle or each dose (10, 20, 30, or 60 mg/kg, i.p.) of sildenafil once 1 h before the FST. Sildenafil dose-dependently reduced the duration of immobility: no effect at 10 or 20 mg/kg and a significant reduction at 30 and 60 mg/kg (Fig. 1a). The effect of successive treatments with 20 mg/kg of sildenafil on the depression-related behavior in WT mice was examined next. Mice were injected with sildenafil every 24 h for 3 days and then given the FST (Fig. 1b). Successive injections of 20 mg/kg of sildenafil reduced the duration of immobility. Also investigated was whether 60 mg/kg of sildenafil affected mating behavior in male mice. However, the drug had no effect on mating (data not shown).

Inhibition of the antidepressant-like effect of sildenafil by the blockade of OTR

To investigate whether the OT signaling pathway was involved in the antidepressant-like effect of sildenafil, mice were co-administered 60 mg/kg of sildenafil and 80 mg/kg of atosiban, an OTR antagonist, and given the FST. Atosiban alone had no effect on the duration of the immobility of the mice but inhibited the decrease in the duration of immobility caused by sildenafil (Fig. 2a). We confirmed the involvement of the OTR signaling pathway in the antidepressant-like effect of sildenafil using male OTR KO mice. Sildenafil had no effect on immobility time in the KO mice, whereas the drug significantly inhibited immobility time in WT mice (Fig. 2b). To exclude the possibility that sildenafil and atosiban affect locomotor activity, we examined the effect of the drugs on WT males in an open-field test.

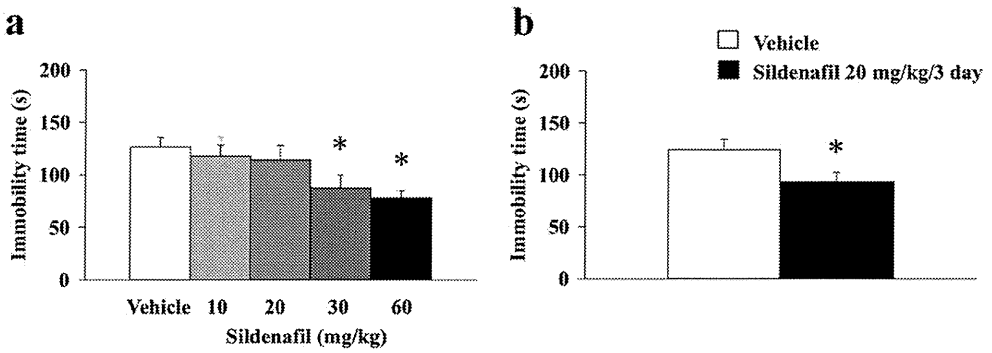

Fig. 1. Antidepressant-like effect of sildenafil in male mice. (a) Male mice were administered vehicle (i.p., $n=7$) or a concentration of sildenafil (i.p., $n=6–7$). After 1 h, the FST was given and immobility time was measured. * $P<0.05$ (one-way ANOVA followed by Tukey–Kramer's post hoc test). (b) Effect of successive administrations of a low dose of sildenafil. Male mice were administered vehicle (i.p., $n=8$) or sildenafil (20 mg/kg/3 d, i.p., $n=8$) every 24 h for 3 d. Mice were given the FST 1 h after the last administration of sildenafil. Data are expressed as the mean±SEM. * $P<0.05$ (Student's t-test).

Neither drug affected the total distance covered by the mice (Fig. 2c). We also compared the locomotor activity of OTR KO mice with that of WT mice. The locomotor activity of OTR KO mice was the same as that of WT mice (Total distance of WT and OTR KO mice; 2506±198 and 2647±201, $P>0.05$ by Student t-test, $n=5$ each).

Induction of CREB phosphorylation by sildenafil and the effect of a MEK inhibitor on the antidepressant-like effect of sildenafil

Increases in neurogenesis, plasticity, and neural survival through the activation of a MAP kinase cascade and subsequent enhanced phosphorylation of CREB in the hippocampus have been proposed as common mediators of antidepressant efficacy (D'Sa and Duman, 2002; Gourley et al., 2008; Duric et al., 2010). OT induced the phosphorylation of CREB through activation of MAP kinase signaling in the hippocampus (Tomizawa et al., 2003). The present and previous results suggest that both the activation and subsequent phosphorylation were induced by sildenafil through the secretion of OT, resulting in the antidepressant-like effect. To test this hypothesis, it was examined whether sildenafil induced the phosphorylation of CREB in the hippocampus of male mice. Sildenafil increased the phosphorylation of CREB compared with vehicle, and atosiban inhibited the sildenafil-induced phosphorylation (Fig. 3a). Moreover, sildenafil had no effect on CREB phosphorylation in OTR KO mice (Fig. 3b).

To investigate the involvement of MAP kinase signaling in the antidepressant-like effect of sildenafil, we examined whether an MEK inhibitor, PD18461, inhibited the effect. PD18461 attenuated the reduction in immobility time caused by sildenafil in male mice (Fig. 4) but had no effect on locomotor activity in the mice (total distance of mice treated with vehicle and PD18461; 2326±176 and 2403±150, $P>0.05$ by Student t-test, $n=5$ each).

DISCUSSION

The present study provided the following three important findings. First, sildenafil had an antidepressant-like effect. Second, the effect was inhibited by blockade of the OTR. Third, sildenafil activated MAP kinase signaling and induced the subsequent phosphorylation of CREB via an OT-mediated signaling pathway.

The large number of brain neuropeptides, characterized by discrete sites of synthesis and multiple receptors, represent likely research candidates for novel therapeutic targets for MDD (Slattery and Neumann, 2010). Notably, preclinical and clinical studies have shown OT to be a prominent candidate. For instance, an increased concentration of OT in plasma is negatively correlated with symptoms of depression (Scantamburlo et al., 2007), and plasma OT levels are significantly lower in patients with major depression at night, when the influence of daily activities is reduced (Frasch et al., 1995). Moreover, OT produced a robust reduction in immobility during the FST in male mice (Arletti and Bertolini, 1987; Ring et al., 2010). Although these studies have provided valuable insights into OT as a potential therapeutic for MDD, problems exist (e.g. metabolic instability, short half-life, and poor BBB penetration), regarding the ultimate utility of synthetic OT (Ermisch et al., 1985). The present and previous results (Brink et al., 2008; Liebenberg et al., 2010a,b, 2011) showed that sildenafil had an antidepressant-like effect via OT signaling. Sildenafil is widely used to treat erectile dysfunction and pulmonary arterial hypertension and can be administered orally (Francis and Corbin, 2005). Moreover, sexual dysfunction is a common adverse effect of antidepressants, selective and nonselective serotonin reuptake inhibitors, that frequently results in treatment noncompliance (Harrison et al., 1986; Montejo et al., 2001). A randomized controlled study showed that sildenafil effectively improved erectile function and other aspects of sexual function in men with sexual dysfunction associated with the use of antidepressants (Nurnberg et al., 2003). These results suggest that sildenafil may become a promising antidepressant without the side effect of sexual dysfunction.

Sildenafil is a selective inhibitor of phosphodiesterase type 5, the enzyme responsible for the degradation of cGMP, thereby enhancing cGMP signaling (Puzzo et al.,

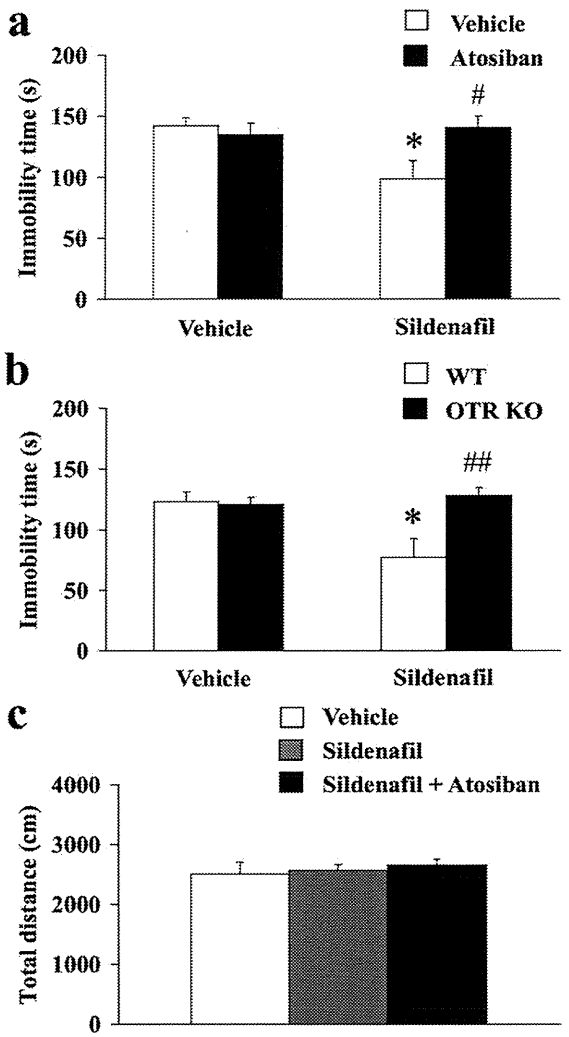

Fig. 2. Effect of a blockade of OTRs on the antidepressant-like effect of sildenafil in male mice. (a) Effect of atosiban, an OTR antagonist. Males were separated into three groups and administered vehicle (i.p., $n=5$), atosiban (80 mg/kg, i.p., $n=6$), sildenafil (60 mg/kg, i.p., $n=6$), or sildenafil (60 mg/kg)+atosiban (80 mg/kg, i.p., $n=6$). Mice were given the FST 1 h after the administration of each drug. * $P<0.05$ compared with sildenafil+atosiban (two-way ANOVA followed by Tukey–Kramer's post hoc test). (b) Effect of sildenafil in OTR-deficient mice. WT and OTR KO males were intraperitoneally administered vehicle and sildenafil (60 mg/kg), then given the FST 1 h later. $n=6$ each. * $P<0.05$ compared with the control (vehicle), ## $P<0.01$ when comparing WT sildenafil vs. OTR KO sildenafil (two-way ANOVA followed by Tukey–Kramer's post hoc test). (c) Total locomotor activity in male mice. WT male mice were administered vehicle, 60 mg/kg of sildenafil and 80 mg/kg of atosiban 1 h before the test, and then subjected to an open-field test. Data are expressed as the mean±SEM. $n=8$ each. A two-way ANOVA followed by Tukey–Kramer's post hoc analysis was used to compare each condition.

2008). cGMP is one of the targets for the action of nitric oxide (NO) (Puzzo et al., 2008). NO–cGMP signaling is involved in various cognitive and emotional processes including depressant-like behavior (Puzzo et al., 2008) and affective disorders (Harvey, 1996). Moreover, NO synthase inhibitors have antidepressant-like properties. These results suggest that sildenafil may increase the secretion of OT through the activation of NO-cGMP signaling.

The present study showed that a lower dose (10 mg/kg) of sildenafil had no antidepressant-like effect, and consistent with previous findings that immobility in the FST was not changed significantly in rats treated with 10 mg/kg of sildenafil alone (Brink et al., 2008; Liebenberg et al., 2010a,b). The doses (5–10 mg/kg) employed cover the range of those used for the clinical treatment of erectile dysfunction. The reason why the dose used clinically has no antidepressant-like effect is unclear. One possibility is that it may be difficult for sildenafil to cross the blood–brain barrier. Indeed the administration of 60 mg/kg but not 10 mg/kg of sildenafil raised OT levels in the PVN of mice (data not shown). For clinical use in the treatment of MDD, it is necessary to lower the effective dose of sildenafil. Previous studies in rats showed that sidenafil (10 mg/kg) significantly decreased immobility time in the FST in combination with a muscarinic acetylcholine (mACh) receptor antagonist (atropine) (Brink et al., 2008; Liebenberg et al., 2010a). These results suggest that atropine may reveal underlying antidepressant-like activity of sildenafil, and anticholinergic bolstering of this activity of sildenafil may become a new treatment strategy for depression.

In contrast, a low dose of sildenafil (5 mg/kg) inhibits the antidepressant-like effect of some drugs such as folic acid, a water-soluble vitamin (Brocardo et al., 2008), tramadol, a synthetic opioid (Jesse et al., 2008), lithium (Ghasemi et al., 2008) and escitalopram, a serotonin reuptake inhibitor (Zomkowski et al., 2010) even though the same dose of sildenafil alone had no effect on immobility time in the FST (Brocardo et al., 2008; Jesse et al., 2008; Ghasemi et al., 2008; Zomkowski et al., 2010). Although the precise mechanisms on the inhibitory effect of a low dose of sildenafil are unknown, the dose of sildenafil may be crucial for the antidepressant effect. Further study to investigate whether higher doses (30–60 mg/kg) of sildenafil affect the antidepressant-like effect of the drugs is needed. The reverse effect of sildenafil is an issue for the clinical use as an antidepressant. It is also important to clarify the precise mechanism of the reverse effect.

Although the exact cellular and molecular mechanism underlying the pathophysiology of MDD has not been identified, brain imaging and postmortem studies have provided evidence of changes in the cellular architecture of several limbic regions, most notably atrophy of hippocampal pyramidal neurons and a corresponding reduction in the volume of the hippocampus, in patients with MDD (Sheline et al., 1996, 2003; Stockmeier et al., 2004). Such alterations to the structure and function of the hippocampus could contribute to certain aspects of MDD, including disruption of cognition, depressed mood, feelings of helplessness, anhedonia, and control of the hypothalamic-pituitary-adrenal axis (McEwen 1999; Drevets 2000, 2001). Increases in neurogenesis, plasticity, and neural survival through the activation of a MAP kinase cascade and subsequent enhanced phosphorylation of CREB in the hippocampus have been proposed as common mediators of

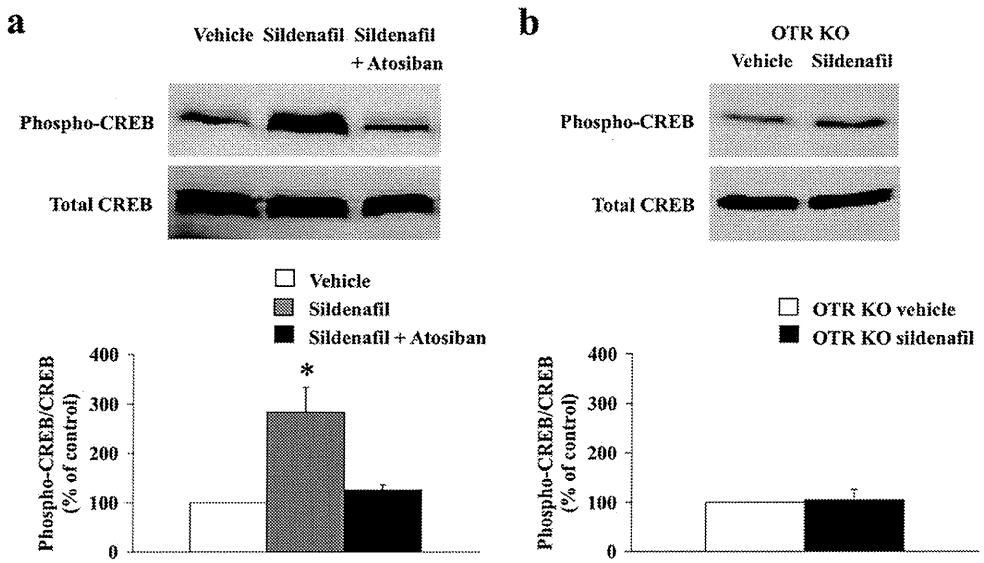

Fig. 3. Effect of sildenafil on CREB phosphorylation in the hippocampus of WT (a) and OTR KO (b) male mice. Vehicle, sildenafil (60 mg/kg), and sildenafil+atosiban (80 mg/kg) were administered intraperitoneally, and hippocampi were dissected 30 min later. The hippocampi were homogenized with boiled 1% SDS, and Western blotting was performed using anti–phospho-CREB and anti-total CREB antibodies. Upper panel, representative results of Western blotting. Lower panel, quantitative analysis of the level of phospho-CREB. The level of phospho-CREB was normalized with the total CREB level in each sample. Data are expressed as the mean±SEM. n=3 each. * P<0.01 vs. vehicle only (one-way ANOVA followed by Tukey–Kramer's post hoc test).

antidepressant efficacy (D'Sa and Duman, 2002; Gourley et al., 2008; Duric et al., 2010). We previously showed that OT induced the phosphorylation of CREB through activation of MAP kinase signaling i and enhanced neural plasticity in the hippocampus (Tomizawa et al., 2003). Moreover, sildenafil induces neurogenesis (Zhang et al., 2002, 2006a,b). These results suggest the increase in the secretion of OT and phosphorylation of CREB by MEK in the hippocampus to be the molecular mechanism behind the antidepressant-like effect of sildenafil.

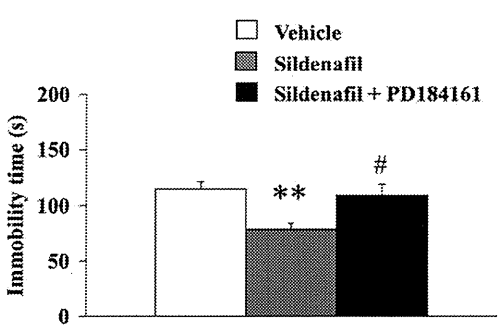

Fig. 4. Effect of PD184161 on the antidepressant-like effect of sildenafil in male mice. Males were intraperitoneally injected with PD184161 (30 mg/kg, i.p.) or vehicle and then administered sildenafil 10 min later. Mice were given the FST 60 min after the sildenafil administration. Data are expressed as the mean±SEM. n=5–8. ** P<0.01 compared with the control (vehicle), # P<0.05 when comparing sildenafil vs. sildenafil+PD184161 (one-way ANOVA followed by Tukey–Kramer's post hoc test).

CONCLUSION

In conclusion, the present results suggest sildenafil to have an antidepressant-like effect through the activation of OT signaling and to be a promising drug for the treatment of depression.

Acknowledgments—This work was supported by a grant-in-aid for Scientific Research on Priority Areas—System study on higher-order brain functions-from the Ministry of Education, Culture, Sports, Science and Technology of Japan and by a grant-in-aid for Scientific Research from the Ministry of Health, Labour and Welfare of Japan.

REFERENCES

Argiolas A, Gessa GL (1991) Central functions of oxytocin. Neurosci Biobehav Rev 15:217–231.

Arletti R, Bertolini A (1987) Oxytocin acts as an antidepressant in two animal models of depression. Life Sci 41:1725–1730.

Bielsky IF, Young LJ (2004) Oxytocin, vasopressin, and social recognition in mammals. Peptides 25:1565–1574.

Boolell M, Gepi-Attee S, Gingell JC, Allen MJ (1996) Sildenafil, a novel effective oral therapy for male erectile dysfunction. Br J Urol 78:257–261.

Brink CB, Clapton JD, Eagar BE, Harvey BH (2008) Appearance of antidepressant-like effect by sildenafil in rats after central muscarinic receptor blockade: evidence from behavioural and neuroreceptor studies. J Neural Transm 115:117–125.

Brocardo Pde S, Budni J, Lobato KR, Kaster MP, Rodrigues AL (2008) Antidepressant-like effect of folic acid: involvement of NMDA receptors and L-arginine-nitric oxide-cyclic guanosine monophosphate pathway. Eur J Pharmacol 598:37–42.

D'Sa C, Duman RS (2002) Antidepressants and neuroplasticity. Bipolar Disord 4:183–194.